REPUBLIC OF TÜRKİYE
KIRŞEHİR AHİ EVRAN UNIVERSITY
INSTITUTE OF NATURAL AND APPLIED SCIENCES
DEPARTMENT OF MECHANICAL ENGINEERING

DESIGN OF AN AXISYMMETRIC TRIANGULAR HEATSINK WITH RADIAL ARRANGEMENT AND EXPERIMENTAL INVESTIGATION OF NATURAL CONVECTION HEAT TRANSFER

JAMAL BAKR KHALEEL KHALEEL

MSc THESIS

KIRŞEHİR
2024

REPUBLIC OF TÜRKİYE
KIRŞEHİR AHİ EVRAN UNIVERSITY
INSTITUTE OF NATURAL AND APPLIED SCIENCES
DEPARTMENT OF MECHANICAL ENGINEERING

DESIGN OF AN AXISYMMETRIC TRIANGULAR HEATSINK WITH RADIAL ARRANGEMENT AND EXPERIMENTAL INVESTIGATION OF NATURAL CONVECTION HEAT TRANSFER

JAMAL BAKR KHALEEL KHALEEL

MSc THESIS

Supervisor
Asst. Prof. Dr. Merdin DANIŞMAZ
II. Supervisor
Prof. Dr. Tahseen Ahmed TAHSEEN

KIRŞEHİR
2024

KIRŞEHİR AHİ EVRAN UNIVERSITY

INSTITUTE OF NATURAL AND APPLIED SCIENCES

MSc THESIS

ETHICS DECLARATION

In this thesis study, which I have read and understood the Kırşehir Ahi Evran University Scientific Research and Publication Ethics Directive and which I have prepared in accordance with the Kırşehir Ahi Evran University Institute of Natural and Applied Science Thesis Writing Rules;

- I have obtained the data, information, and documents I have presented in the thesis within the framework of academic and ethical rules,
- I present all information, documents, evaluations, and results in accordance with scientific ethical rules,
- I have cited all the works I have benefited from in the thesis by making appropriate references,
- I have not made any changes in the data used and the results,
- This study, which I have presented as a thesis, is original,

Otherwise, I declare that I accept all legal actions to be taken against me in this regard and all loss of rights that may arise against me. ...../……. /2024

Student

JAMAL BAKR

KHALEEL KHALEEL

LIST OF CONTENTS

Page No

LIST OF CONTENTS ..... **I**
ACKNOWLEDGEMENTS ..... **III**
GENİŞLETİLMİŞ ÖZET ..... **IV**
ABSTRACT ..... **VI**
LIST OF TABLES ..... **VII**
LIST OF FIGURES ..... **VIII**
LIST OF ICONS AND ABBREVIATIONS ..... **X**
1. INTRODUCTION **1**
1.1. Heat Transfer through Extended Surfaces 2
1.2. Heat Transfer Enhancement 3
1.3. The Heat Sink 4
1.4. The Fin Shape 5
1.5. The Fin Design 6
1.6. Radial Fins and Modern Applications 7
1.7. Study Objectives 10
2. LITERATURE REVIEW **11**
2.1. Introduction 11
2.2. Comprehensive Review 11
2.3. Subject of The Current Study 31
3. MATERIAL AND METHOD **33**
3.1. Introduction 33
3.2. Current Research Strategy 33
3.3. Experimental Setup 34
3.4. Materials 36
3.4.1. Cylinder (Fin Base) 36
3.4.2. Fins 39
3.4.3. Temperature Measurements 42
3.4.4. Voltage Regulator 43
3.4.5. Electrical Heaters 43
3.4.6. Electric Current and Voltage Measurement 44
3.4.7. Thermocouple 45
3.5. Thermocouple Calibration 46
3.6. Methods 46

3.6.1. Components of The System 46
3.6.2. Test Preparation Procedure 47
3.6.3. Test and Calculation Mechanism 47
3.6.4. The Study Cases 49
3.7. Data Reduction 50
4. RESULT AND DISCUSSIONS 55
4.1. Introduction 55
4.2. Relationship of Change in Power Supplied (Thermal Flow) on Temperature Behavior 55
4.3. Thermal Resistance 58
4.4. Nusselt Number 59
4.5. Developing The Correlation Equation 59
4.6. A sample of calculation 66
5. CONCLUSION AND RECOMMENDATIONS 69
5.1. Conclusion 69
5.2. Recommendations 70
6. REFERENCES 71
CURRICULUM VITAE 79

ACKNOWLEDGEMENTS

I wish to convey my profound appreciation to my renowned supervisors, Assistant Professor Dr. Merdin DANIŞMAZ and Professor Dr. Tahseen Ahmed TAHSEEN., whose unwavering support, insightful guidance, and invaluable mentorship have been instrumental throughout the journey of my master's studies. Their profound knowledge, motivation, and unwavering dedication to achieving high academic standards have greatly enhanced my research journey and played a pivotal role in the effective culmination of this thesis.

I extend my heartfelt thanks to the Department of Mechanical Engineering for providing a conducive academic environment and resources essential for my research endeavors. The stimulating atmosphere and collaborative spirit within the department have greatly enhanced the quality of my academic journey.

I am also grateful to my peers and colleagues for their camaraderie and intellectual exchange, which have played a crucial role in shaping my ideas and refining my work.

This academic journey has been a fulfilling and transformative experience, and I am thankful for the support and encouragement I have received from all those who have been part of this endeavor.

I dedicate my thesis to my family.

January , 2024 Jamal Bakr KHALEEL KHALEEL

GENİŞLETİLMİŞ ÖZET

YÜKSEK LİSANS TEZİ

RADYAL YERLEŞIMDE EKSENEL SIMETRIK ÜÇGEN KANATÇIKLI SOĞUTUCU TASARIMI VE DOĞAL TAŞINIMLA ISI TRANSFERININ DENEYSEL İNCELEMESI

JAMAL BAKR KHALEEL KHALEEL

KIRŞEHİR AHİ EVRAN UNIVERSITY
INSTITUTE OF NATURAL AND APPLIED SCIENCES
DEPARTMENT OF MECHANICAL ENGINEERING

Danışman:	**Dr. Öğr. Üyesi Merdin DANIŞMAZ**
	Yıl: 2024 Sayfa: 77
Jüri:	**Dr. Öğr. Üyesi Merdin DANIŞMAZ**
	Prof. Dr. Levent URTEKİN
	Prof. Dr. Ali Osman KURBAN
	Asst. Prof. Dr. Omer Adil ZAINAL
İkinci Danışman	**Prof. Dr. Tahseen Ahmed TAHSEEN**

Yarı iletken teknolojisindeki muazzam ve son gelişmelerin bir sonucu olarak, mikro elektronik ekipmanın ısı üretim yoğunluğunda (termal akış) belirgin bir artış olmuştur. Bu elektronik cihazların ısı üretimi, sürekli olarak en iyi şekilde performans göstermeleri için talepte bulundukları ve bu cihazların ölçeklendirilmesine ek olarak maliyetinin düşük olduğu için önemli ölçüde artmıştır. Mesela silikonun mikroişlemcilerinden ısı üretme (termal akış) yoğunluğu 100 W/m2ye ulaştı ve bu termal akış Güneş yüzeyinde ona yaklaştı. Elektronik cihazın performansı ve güvenilirliği, yukarıda uygulanan ısı üretim yoğunluğundan kaynaklanan bağlantı sıcaklığındaki bir artıştan olumsuz yönde etkilenir. Örneğin, bağlantı sıcaklığı arttıkça, ışık yayan lamba (LED) verimliliği önemli ölçüde azalır. Bu nedenle, bu elektronik bileşenlerin çalışmasının işleyişini ve güvenilirliğini geliştirmek için etkili soğutma mekanizması gereklidir. Doğal yüke sahip termal dağılımların sadeliği, güvenilirliği ve düşük uzun vadeli üretim maliyeti nedeniyle uygun olduğu kanıtlanmış bir dizi soğutma yöntemi önerdim. Bu nedenle, ışık yayan lambaları soğutmak için yaygın olarak kullanılan dikey (radyal) kanatlı silindirik ısı dikkat dağıtıcıları son zamanlarda kullanılmıştır. Ek olarak, ısı iletim alanını artırarak ısı infüzyonunu teşvik etmek amacıyla radyal termal dikkat dağıtıcıların kullanılması. Serbest yük ısı iletim koşulları altında termal performansı arttırmak için yeni kanatçık formları kullanılır. Radyotermal distraksiyonlar, ısı iletiminin yüzey alanını arttırdıkları için ısı iletimini teşvik etmek için ekipman olarak kullanılır. Bu, serbest termal yük ile ısı iletim koşullarında termal performansı artırmak için yeni kanatçık formları kullanılarak yapılır. Mevcut araştırma, üçgen olan ve radyal termal dikkat dağıtıcılarda termal performans üzerinde etkisi olan yeni bir yüzgeç formunu vurgulamaktadır. Yük ısı transfer katsayısını nasıl etkilediğini görmek için bu araştırmada üçgen şekil alanı değiştirilirse. Test sistemi, çapı (70 mm) ve uzunluğu (210 mm) olan dairesel şekilli alüminyum metalden yapılmış katı bir silindirden oluşur, ve silindirin üst güvertesinde deliklerin kuvvetsiz olması

için uzunluk boyunca çap (8 mm) ve derin (200 mm) beş delik çalıştırıldı. Fin taban silindirinin üst yüzeyinin delinmesi, silindirin merkezinin (R = 35mm) ilk deliği ve ardından diğer dördünü delmeye karar vermesinden sonra gerçekleştirildi silindirin merkezinden uzaklığı (17,5 mm) ve bu deliklere yerleştirilecek bir açıyla (90°) belirlenerek delikler belirlendi. Bir dere kalınlığında (3 mm) şeklinde on iki uzunlamasına kesiler yaptık, silindirin dış yüzeyi boyunca kanatçıkları stabilize etmek için derin (3 mm) ve uzun (210 mm), bir kesi ile diğeri arasındaki açının (30°) olduğunu bilmek.

Çeşitli termal çift tiplerini kullanan 24 kanallı Cihaz Çok Kanallı Sıcaklık Ölçer AT 4524 tipi sıcaklık kaydedici (24 kanal), cihazın doğruluğunu kullanın (% 0.2% + 1 °C) ve okuma aralığı °C (-200) ila (1300). Bu araştırmada, dördü farklı yerlerdeki yüzgeçlerden birinde ve üçü silindirin gövdesinde olmak üzere dört tanesinin sıcaklığını ölçmek için sekiz saha kurulmuştur. Çalışma, ilave ısı miktarı 20.16, 66.03, 105.30, 157.62, 196.08 W olmak üzere beş oran için yapılmıştır. Yüzgeç yüksekliği, uzunluğu, gibi geometrik işlemlere bağlı bir dizi yavru bulmak için bir ilişki geliştirilmiştir, yüzgeçler arasındaki mesafe artı Riley numarası ile temsil edilen akan sıcaklık oranının etkisi. Çalışma vakaları da üç vakaya (Case I: Fin Drop = 15 mm, Case II: Fin Drop = 35 mm, ve Case III'e ayrıldı: Fin Damlası = 55 mm). Sonuçlar, sıcaklık farkının (III) durumunda diğer iki duruma göre daha yüksek olduğunu göstermiştir. Ocuk sayısı, sıcaklığı artırarak yavru sayısının arttığını ve ilk vakanın diğer vakalara kıyasla en iyi yavru sayısı olduğunu göstermektedir. Isıl direnç gelince, termal taşmayı artırarak azalır ve en düşük sıcaklık dayanımı değerleri diğer vakalara kıyasla üçüncü örnekte (III) idi. Mevcut sonuçlar, ilk durumda yüzgecin ısı iletimini, ikinci ve üçüncü vakalara kıyasla sırasıyla Riley'in yüksek sayısında %12,07 ve %30'a kadar dağıttığını göstermektedir. Riley sayısının maksimum değerindeki birinci ve ikinci ardışık vakalara kıyasla III. durumda termal direnç %13,91 ve %16,23'e düşmüştür. Korelasyon katsayısına gelince, değeri (R^2= 97%) ve ±% 5'i geçmeyen bir çizgi oranıdan daha az değildir%. Yukarıdakilere dayanarak, bu tür termal sistemlerin geometrik tasarımları bu geliştirilmiş konfigürasyonlardan yararlanabilir. Bu çalışmanın sonuçlarının, LED ampuller için üçgen kanatlı radyal termal lavabonun tasarımı için yararlı olması beklenmektedir, yanı sıra birçok mühendislik uygulamaları için bu tarz radyasyon termal radyasyon tasarımı.

Anahtar Kelimeler: Radial ısı emiciler, Serbest konveksiyon ısı transferi, Yeni kanat şekilleri, Termal performans, Isı tedarik oranları.

ABSTRACT

MASTER'S THESIS

DESIGN OF AN AXISYMMETRIC TRIANGULAR HEATSINK WITH RADIAL ARRANGEMENT AND EXPERIMENTAL INVESTIGATION OF NATURAL CONVECTION HEAT TRANSFER

JAMAL BAKR KHALEEL

KIRŞEHİR AHİ EVRAN UNIVERSITY
INSTITUTE OF NATURAL AND APPLIED SCIENCES
DEPARTMENT OF MECHANICAL ENGINEERING

Supervisor:	**Dr. Öğr. Üyesi Merdin DANIŞMAZ** **Yıl: 2024 Sayfa: 77**
Jury:	**Dr. Öğr. Üyesi Merdin DANIŞMAZ**
	Prof. Dr. Levent URTEKİN
	Prof. Dr. Ali Osman KURBAN
	Asst. Prof. Dr. Omer Adil ZAINAL
Co-Supervisor	**Prof. Dr. Tahseen Ahmed TAHSEEN**

Radial heat sinks are commonly used to facilitate heat transfer by increasing the surface area available for heat transfer. Novel fin forms are utilized to improve thermal heat performance in the context of convection-free heat transfer. The current work aims to experimentally evaluate the impact of a new fin shape on the thermal behavior of a circular base radial heat sink with. The goal was to determine the optimal reference model by evaluating and comparing the three models of heat sink, I, II, and III. The study investigated the rates at which heat was provided, which were 20.16, 66.03, 105.30, 157.62, and 196.08 W. The current findings demonstrate that the configurations in in case I fin had a heat transfer reduction of 12.07% and 30% compared to case II and case III, respectively, at high Rayleigh numbers. The thermal resistance in example III decreased by 13.91% and 16.23% when compared to case I and case II, respectively, at the maximum value of the Rayleigh number. Subsequently, relying on empirical evidence, a correlation was proposed to calculate the value of the Nusselt number for natural convection from a radial heat sink including vertically aligned double triangular fins. The correlation between the developed Nusselt number and the actual value (experimental) is good agreement, with an accuracy of less than ±5% and a coefficient of determination (R^2) of up to 97%.

Key Words: Radial heat sinks, Free convection heat transfer, Novel fin shapes, Thermal performance, Heat supply rates.

LIST OF TABLES

Page No

Table 3.1: Dimensions of the geometric fin array for the cases under investigation. 50
Table 3.2: An overview of the uncertainty values. 54
Table 4.1: Efficiency values along with fin height and the differences in added heat in the studied cases. 62

LIST OF FIGURES

Page No

Figure 1.1: Hypothetical cooling fins on the Stegosaurus dinosaur (Çengel and Ghajar, 2015)..... **1**
Figure 1.2: Several common instances of extended surfaces: (a) Rectangular fin oriented in the longitudinal direction, (b) rectangular fin on tube surface, (c) inclined rectangular fin, (d) equivalent cut rectangular fin, (e) annular fin, (f) inclined annular fin, (g) constant cross-section. **6**
Figure 1.3: Some examples on radial fins in modern applications (Sadeghianjahromi and Wang, 2021). **9**
Figure 2.1: The circular base and rectangular fins of the radial heat sink (Hanafi *et al*, 2015)..... **13**
Figure 2.2: Configuration of the fins used in the study (Li *et al*, 2016). 13
Figure 2.3: Experimental setup diagram of the pin-fin radial heat sink (Jang *et al*, 2012)..... 14
Figure 2.4: Schematic of the experimental setup platform (Li and Byon, 2016 a). **15**
Figure 2.5: Four-perforated radial heat sink (Li *et al*, 2016). **18**
Figure 2.6: Diagrammatic representation of the heat sink (a) with and (b) without a chimney (Hassan *et al*, 2021). **19**
Figure 2.7: Square, circular in shape, elliptical pin fins, and rectangular plate fins (El Ghandouri, 2020). **21**
Figure 2.8: A photographic image of the heat sink used in this study (Yildiz and Yüncü, 2004)..... 23
Figure 2.9: Photographic images of the heat sink (a) perforated fins, (b) non-perforated fins. 25
Figure 2.10: The application of notched fins in heat dissipation. **27**
Figure 2.11: The use of tapered fin shape to increase maximum heat transfer by (Rao and Somkuwar, 2021). 28
Figure 2.12: Utilizing thermal boundary layers between the fins by (Huang and Chen, 2022)..... 29
Figure 2.13: The cross-fin heat sink design by (Feng *et al*, 2018)..... **29**
Figure 2.14: The Y-shaped heat sink by Huang *et al*. **30**
Figure 2.15: The three designed types of heat sinks with TPMS bases by (Baobaid *et al*, 2022)..... **31**
Figure 3.1: System setup. **35**
Figure 3.2: Illustration depicting the configuration of the experimental arrangement. **36**
Figure 3.3: Photographs of the cylinder with drilled holes. **37**
Figure 3.4: Cylinder base schematic illustration with dimensions specified in millimeters... **38**
Figure 3.5: Photographs of the base cylinder with thermocouples fixed and electric heaters assembly. **38**
Figure 3.6: The 3D design of the selected fins. **39**
Figure 3.7: Photographs of the fins used in this study. (a) The fin with drop 15 mm in the middle. (b) The fin with drop 35 mm in the middle. (c) The fin with drop 55 mm in the middle. **41**
Figure 3.8: Schematic diagram of fins installation on the cylinder surface. **41**
Figure 3. *3*9.: Three-dimensional diagram of fins after being attached to the cylinder base with their dimensions. **42**
Figure 3.10: TC-08 program interface. **43**
Figure 3.11: Voltage Regulator Device. **43**
Figure 3.12: Cartridge heaters using in this study. **44**

Figure 3.13: Multi-meter device for voltage and current readings. **44**
Figure 3.14: Thermocouple Type K used in the experimental work. **45**
Figure 3.15: Thermocouples locations. **45**
Figure 3.16: Thermocouple calibration. **46**
Figure 3.17: Double triangle fin. **50**
Figure 4.1: Temperature profiles analyzed for various fin heights and heat inputs in three different scenarios. **56**
Figure 4.2: The effect of fin height on temperature distribution in three studied cases. **57**
Figure 4.3: Examining the relationship between the heat sink's Nusselt number and the Rayleigh number under various conditions is the goal of this investigation. **58**
Figure 4.4: Variation in thermal resistance based on heat flow at several cases. **59**
Figure 4.5: Comparison of the anticipated Nusselt numbers derived from the modified correlation with the measured Nusselt numbers acquired from experimental data. **62**

LIST OF ICONS AND ABBREVIATIONS

Icons		Description
A	:	Area
c_p	:	Specific heat capacity
d	:	Exploration diameter
D	:	Diameter of fin base cylinder
F	:	Form factor
g	:	Ground acceleration
h	:	Heat transfer coefficient by convection
H	:	Fin length
k	:	Thermal conductivity
L	:	Fin length
I	:	current
m	:	mass
n	:	Number of holes
N	:	Number of fins
Q	:	Equipped capacity
R_{th}	:	Thermal resistance
t	:	Fin thickness
T	:	Temperature
v	:	Volume
		Nondimensional symbols
El	:	Elenbaas
Ra	:	Rayleigh number
Nu	:	Nusselt number
		Greek symbols
α	:	Thermal diffusivity
β	:	Volumetric expansion coefficient
$\mathcal{E}$	:	Emissivity
μ	:	viscosity
ν	:	Kinematic viscosity
ρ	:	Density
σ	:	Stefan-Boltzmann constant $5.670*10^{-8}$
ϕ	:	Voltages
Al	:	Aluminum
b	:	Fin base
$Act.$	:	Actual
φ	:	air

1. INTRODUCTION

Fins emerged as a fascinating adaptation some 150 million years ago, during the Jurassic epoch, as shown in Figure (1.1). The Stegosaurus, a dinosaur of this era, possessed two parallel rows of prominent and peculiar bone plates running down its dorsal region. Scientists formerly held the belief that these plates served as a form of protective armor against other predators. It has been discovered that a substantial amount of blood circulates through these structures, and they may have functioned similarly to a car radiator. The heart propels blood through the vessels, while the plates function as heat-dissipating fins to regulate the temperature of the circulating blood (Çengel and Ghajar, 2015).

Figure 1.1: Hypothetical cooling fins on the Stegosaurus dinosaur (Çengel and Ghajar, 2015).

To improve heat transmission between the solid surface and the fluid that surrounds it, thermal dissipation through expanded areas and fins is a technique utilized, such as air or water (Shah, 2011). The purpose of extended surfaces is to improve the efficiency of various systems and equipment, such as electrical appliances, by reducing the temperature gradient and increasing the rate of heat transfer, electronics, and industrial heat exchangers (Može *et al*, 2020). Because heat transfer via natural convection has so many applications in so many different areas, it is considered a very important topic. Natural convection currents are formed within the fluid due to buoyancy force effects, even though there is no applied velocity or force that causes this type of load. In order for devices that use multiple heat transfer mechanisms to function and be designed properly, natural convection is essential. It significantly affects running

costs and heat transfer rates, making it a preferred choice over forced convection in many cases (Bejan, 2013). Starting from the exploration of space that began in the early 1960's, the radiating surface with fins in the form of tubular sheets and annular fins radially became a common design feature for heat dissipation systems in spacecraft. Over the past thirty years, the finned heat sink has proven to be an effective means of dissipating heat from electronic systems and thus ensuring reliable operation under conditions of extreme heat generation. With the continued growth of extended surface technology, new design ideas continue to emerge, including fins made of slotted plates or special composites and porous media (Schnurr and Cothran, 1974; Aziz, 2006). There is a growing interest among several engineering fields in energy transformations that necessitate rapid heat transfer. As a result, there is a rising need for heat transfer components that exhibit high performance and possess appropriate characteristics in terms of weight, size, cost, and shape. When designing and building heat transfer equipment, we utilize basic shapes and materials including cylinders, pipelines exposed to fluids, and plates to facilitate the movement of heat between sources and sinks. They provide well-known heat absorption or dissipation surfaces called "prime surfaces." To avoid the problem of high load resistance between the main surface and the surrounding fluid, which reduces the overall heat transfer coefficient of the surrounding fluid, the surface area is extended by adding additional surfaces to the main surface (Bergman *et al*, 2011). Biofilm formation by this species increases the high resistance to antibiotics, including fluoroquinolones, beta-lactams, and carbapenems, and this barrier decreases the possibility of bacteria penetrating the immune cell of biofilms and of antibiotics and acts as adequate protection against the host immune systems and antibiotic agents, which leads to continuous colonization of the organism. Treating burn wound bacterial pathogens is a significant challenge, and new methods of reducing death rates associated with bacterial infections in burn injuries are needed (Shariati *et al*., 2019). The emergence of resistance in treatment, which is proved to duplicate the time of hospitalization and total cost of patient care, is even more troublesome (Jindal *et al*., 2015).

1.1.Heat Transfer through Extended Surfaces

When it's necessary to enhance heat transfer from surfaces to the cooling fluid in contact with them in order to maintain these surfaces operating within allowable

temperature limits, extended surfaces are frequently employed in a variety of industrial applications. One element of high-performance heat transfer in relation to these processes and how they behave in a range of temperature settings is heat transfer via extended surfaces. In heat transfer systems, fins or expanded surfaces are employed to enhance the surface area. Commonly used fin forms include triangle, wedge-shaped, annular, straight (rectangular), stretched from a flat wall, and triangular. These standard elements are included in diverse applications, including vehicles, airplanes, and spacecrafts, as well as in chemical processes, cooling of electrical and electronic equipment, thermal ovens, gas turbines, and many other applications. Straight fins are often used to enhance cooling in automobile engines and electric transformers, while annular fins are added to heat exchanger tubes on a wide scale to cool fluids, where the heat exchanger consists of several finned tubes with a fan that pushes large amounts of air through the fins to cool the hot fluid-carrying tubes. The effectiveness of the cooling procedure often relies on the surface area available for heat transfer, which is greatly increased by the presence of fins. The ideal configuration of the heat exchanger, which is composed of tubes with fins depends on other factors such as the external airflow rate, fluid properties, and manufacturing cost. They provide surfaces that absorb or dissipate heat, each of the primary surface is referred to be such when it is expanded by closely associated appendages, such as metal bands and fins on tubes. Extended surfaces, also known as fins, are commonly employed in engineering applications to enhance heat transfer from surfaces to the cooling fluid they encounter. This is done to guarantee that these surfaces remain within acceptable temperature ranges throughout operation (Kraus, 1958).

1.2.Heat Transfer Enhancement

In the field of engineering thermodynamics, it is necessary to design and dimension heat transfer systems in order to produce, transport, or dissipate the necessary quantity of heat. The efficient and secure functioning of heat transfer modules relies on certain prerequisites, such as the targeted cooling and/or heating of particular parts or partition walls inside these systems. These parts can be cooled by continuously reject heat from them at an appropriate rate in electrical systems. Generated heat may cause some problems such as combustion or temperature increase beyond the permissible limit, which may lead to damage or malfunction of the system components, system shutdown, and costly damages. Therefore, in many applications, more emphasis

must be placed on analyzing and testing heat dissipation by providing an effective cooling system to protect equipment from temperature rise problems (Webb and Kim, 2005). In most cases, poorly designed heat transfer systems suffer from surface temperature increases beyond the permissible limit, and these surfaces are unable to dissipate the required amount of unwanted heat. As a result, these surfaces will experience permanent temperature increases and have a detrimental effect on the system. To avoid the harmful effects of temperature, increases on these surfaces, heat must be efficiently removed at the required rates from these surfaces. Generally, heat transfer performance can be improved through (Garimella *et al.*, 2008; Stellman, 1998):

1. Selecting the suitable placement for hot surfaces inside a confined area, which can be either horizontal, vertical, or inclined, based on the heat transfer direction.
2. Enhancing the thermal conductivity between the high-temperature surface and its environment.
3. Using extended surfaces in order to boost the efficient transfer of heat area is a popular way to improve the hot surface's effectiveness in heat transfer.

The fin industry has consistently conducted research to minimize the dimensions, mass, and expenses associated with fins. The size and cost of fins can be reduced by enhancing the heat transfer that fins perform. This improvement can be achieved through the following means (Bejan, 2013):

1. Increasing the fin's surface area relative to its volume in order to improve heat transmission.
2. Improving the fin's coefficient of heat transmission with surrounding materials via surface notch and roughening procedures.
3. Manufacturing fins from materials with high thermal conductivity.

1.3.The Heat Sink

The density of small electronic components in many contemporary electronic circuits is high and cannot be adequately cooled by free convection due to heat-induced floating effects. In order to enhance heat transfer, engineering methods are employed. For example, heat sinks, which have a low thermal resistance and a large effective

surface area, are used to transport heat from a hot surface to the surrounding region. Hence, heat sinks can be defined as "devices or equipment that work to increase heat dissipation from a hot surface". Typically, the coolant medium responsible for dissipating heat in the surrounding environment is air. Typically, the transfer of heat between the solid surface and the cooling air is the least effective within the system, and the interface between the air and solid constitutes the biggest obstacle to heat dissipation. The heat sink principally mitigates this obstacle by augmenting the surface area that comes into direct contact with the coolant. This enables a greater amount of heat to be dispersed and/or lowers the temperature at which the gadget operates. The heat sink's primary job is to control the device's temperature so that it stays below the upper limit that the manufacturer has set (Lee, 1995; Faghri and Zhang, 2006). Heat sinks are affixed directly to the enclosure encompassing semiconductor devices in order to augment the available surface area for the passage of heat from the device itself to the coolant (Lee, 1995), often composed of air. Heat sinks employ diverse fin configurations to enhance the available surface area for efficient heat dissipation. When selecting a suitable heat sink that satisfies the necessary thermal requirements, it is important to take into account many elements that impact both the heat sink's individual performance and the overall system performance. The choice of a particular type of heat sink is largely determined by the external conditions around the heat sink and the heat sink's allowed thermal equilibrium (Bejan, 2013). Certain heat sink Thermal resistance is not a constant value, since it is influenced by several factors such as cooling conditions.

1.4.The Fin Shape

Enhancing the dissipation of generated heat on a surface can be greatly enhanced by strategically positioning fins along the length of the surface, hence augmenting its surface area. These extensions have the ability to assume tangible forms. Figure (1.2) shows examples of the various fin configurations. A planar surface that is fastened to a flat wall is called a straight rectangular fin. The fin may have a consistent cross-sectional area, or it may vary across the length of the fin. Plate fins come in different types: plain, strip, corrugated, pin, and annular fins are those that are circumferentially attached to a cylinder or tube, whose cross-sectional area changes as the radius increases from the cylinder centerline. In contrast, the pin fin is an extended surface

with a circular cross-sectional area that may also have a regular or irregular cross-sectional area (Kraus *et al.*, 2001).

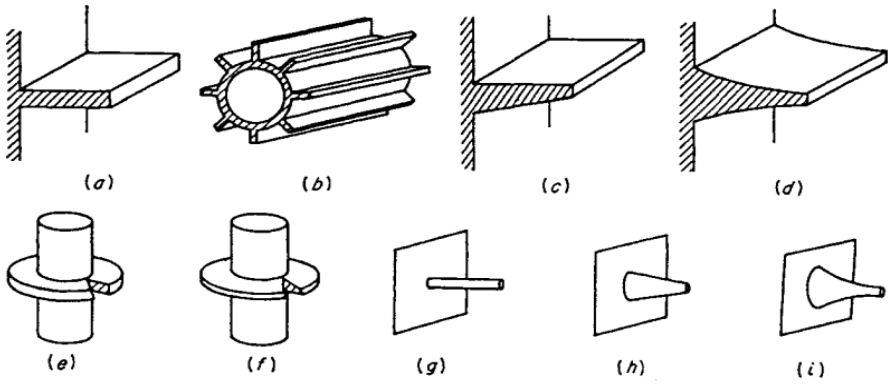

Figure 1.2: Several common instances of extended surfaces: (a) Rectangular fin oriented in the longitudinal direction, (b) rectangular fin on tube surface, (c) inclined rectangular fin, (d) equivalent cut rectangular fin, (e) annular fin, (f) inclined annular fin, (g) Wedge fin of constant cross-section, (h) Wedge fin of conical section, (i) Wedge fin of parabolic section

1.5.The Fin Design

The body surface area is just one of numerous parameters that affect the rate of heat transfer between the flow of fluid and its surroundings. In engineering, it is standard practice to utilize extended surfaces in order to increase the heat transfer rate between the flow of fluid and the surface. One illustration of this is the use of fins to improve the pace at which heat is dissipated as a result of the significant energy required for transmission (Enescu, 2019). When designing a heat exchange system that involves an extended surface, certain equations must be applied for each fin type. The basic heat conduction equation served as the basis for all of these calculations, with specific boundary conditions imposed and simplified in each case. The design of fins is an open matter for improvement, subject to numerous factors that must be taken into follow as (Bejan and Kraus, 2003):

- The additional weight of the fin, which might impact costs or be deemed significant in its own right.
- The impact of the fin on the heat transfer coefficient in the fluid flow surrounding it.
- The spatial arrangement of the channel where the fin is situated.

- The expenses and intricacy involved in producing the fins.
- The pressure decreases due to the utilization of the fin.
- The fin shapes.
- The ideal or incomplete contact with the fin base.
- The heat transfer cases, natural or forced.

Utilizing fins as extended surfaces results in an augmentation of both the weight and dimensions of the system, while concurrently escalating production expenses. Consequently, there has been a significant focus on enhancing fin engineering in recent times, necessitating the utilization of modern methodologies and improved heat transfer equipment. There are two types of heat transfer improvement operations: passive and active (Bergles, 2001). Active techniques require an additional power source in order to enhance or magnify heat transfer, while passive or non-active techniques do not require an external source. Fins are widely utilized to improve heat transmission between a main surface and the surrounding fluid in a variety of industrial applications. They are an effective passive technique that may be deployed for this purpose (Shaeri and Yaghoubi, 2009). Fins are now widely employed as devices to promote heat transfer in the field of prolonged surface technology, which is seeing ongoing expansion and the emergence of novel design concepts, including fins made of composite materials with contrasting properties and porous media, in addition to perforated and serrated fins (Sahin and Demir, 2008). Many studies and research have been conducted to improve the shapes of fins. Further studies have altered the shape by creating incisions in the fin structure, such as chambers, slots, holes, channels, or grooves. This is done in order to maximize heat transfer efficiency or surface area for heat transmission (Kraus *et al*, 2001).

1.6.Radial Fins and Modern Applications

1. Radial fins, which are distinguished by their outward-facing orientation from a central point, are used in a variety of ways in contemporary engineering to improve heat dissipation. The cooling systems of electronic equipment, such computer CPUs and GPUs, are one prominent use. Heat sinks with radial fins provide better thermal performance because they increase the surface area that is accessible for convective heat transfer. For electrical equipment to operate at their best temperatures and

avoid overheating-related problems, effective cooling is essential (Shah, 2011; Alam *et al*, 2020; Umrao Sarwe, 2021).

2. Modern applications that stand for light-emitting diodes, are widely utilized in contemporary applications. Light-emitting diodes (LED) are semiconductor devices that produce light of a certain wavelength when a positive voltage is supplied to a p-n junction. Because light energy at the p-n junction is directly converted into electron energy, LED have a very high energy efficiency and extended lifespan (Jang *et al*, 2012). Lighting technologies using such lamps are continuously being developed. Due to their lack of harmful elements such as mercury and their availability in a diverse array of hues, these lights are utilized in numerous industries. The market for these lamps has recently grown significantly due to improvements in their lighting efficiency and low energy consumption. However, approximately 70% of the lamp's entire energy use is released as heat (Yu *et al*, 2011).

3. Technology is therefore required to increase heat sink performance while lowering bulk (Park *et al*, 2015; Narendran and Gu, 2005). Thus, a radial heat sink might be optimal as LED bulbs often have a round fin shape. Figure (1.3) illustrates some commercial types of LED lamps.

4. Another significant application is in the field of automotive engineering. Radial fins are utilized in the design of heat exchangers, such as radiators and oil coolers, to enhance the overall efficiency of the transfer of heat (Sadeghianjahromi and Wang, 2021). The radial arrangement ensures a larger surface area for the fins exposed to the airflow, promoting more effective cooling of the engine or transmission fluids. This is especially important for improving the performance and longevity of automotive systems (Varma and Gautam, 2022).

5. In the renewable energy sector, radial fins play a role in enhancing the efficiency of solar collectors (Johnston *et al*, 2021). By incorporating radial fins into the design of solar absorbers, engineers can increase the surface area for capturing solar radiation, leading to improved heat absorption and transfer for various solar thermal applications (Kazem *et al*, 2023).

6. Furthermore, radial fins are employed in the design of industrial heat exchangers, where they contribute to the overall effectiveness of heat transfer processes.

Applications range from air conditioning units to chemical processing plants, showcasing the versatility and importance of radial fins in optimizing thermal management.

Figure 1.3: Some examples on radial fins in modern applications (Sadeghianjahromi and Wang, 2021).

1.7. Study Objectives

This study aims at designing novel heat sink that include a new shape of double triangular fin with different middle-waist values, 15, 35, and 55 mm. Through natural heat convection, this design could improve heat dissipation. The following lists the study's aims:

1. Examining how a unique fin shape affects the heat transfer coefficient.
2. Examining the effects of several characteristics, such as Rayleigh number, fin number, and geometric parameters, on the coefficient of heat transmission.
3. The goal is to develop an empirical equation that accurately represents a heat sink with double triangular fins in terms of heat transfer qualities. This formula will take into account the Rayleigh number as well as differences in geometric characteristics, such as the fin's length, thickness, and height.

2. LITERATURE REVIEW

2.1. Introduction

Most of the engineering system will produce heat while it is working. A system overheats, producing heat and ultimately leading to system failure.

The Elenbaas equation is a crucial empirical formula utilized to determine the heat transfer coefficient by free convection from a vertical finned surface (GOV, 2021).

$$\mathrm{Nu} = \frac{1}{24}\mathrm{Ra}^{*}\left[1 - \mathrm{e}^{\left(\frac{-35}{\mathrm{Ra}^{*}}\right)}\right]^{0.75} \qquad (2.1)$$

Where Ra* is Rayleigh's modified number.

Procedures for dissipating high temperatures from a system or component are essential to avert both overheating issues and their detrimental effects (Schuepp, 1973). To estimate the best method for removing heat from a system or component, researchers have conducted several studies and invented many different products. Fins are a type of heat transfer improvement device (Walunj *et al*, 2014) Fins are now commonly utilized in engineering applications, as reported by (Jassem, 2013), to enhance convective heat transfer while minimizing the use of unnecessary surface area. A research conducted by (Dhumne and Farkade, 2013) showed that fins are also frequently used in electrical, power management, and automotive systems. They function as heat management devices, dissipating excess heat from moving or processing systems or even the mechanisms including engine cooling, air conditioning condensers, and refrigeration systems (Dhanadhya *et al*, 2013).

2.2. Comprehensive Review

(Leung *et al*, 1985) have contrasted the thermal efficiency of vertical rectangular fins mounted to a vertical base with that of horizontal fins attached to a vertical base. Research has demonstrated that the configuration of the rectangular fin heat sink significantly affects the efficiency of heat transfer under natural convection settings (Ahmed etr al, 2018; Tari and Mehrtash, 2013), as shown in Figures (2.1) and (2.2). According to investigations conducted by (Kim, 2012; Kim *et al*, 2010), Adjusting the fin's thickness in an orientation perpendicular to the flow of fluid has the ability to reduce heat resistance of up to ten percent. In real-world situations, though, the product's value is determined by the heat sink's size. (Elshafei, 2010) discovered that the

temperature differential between the base plate of these heat sinks and the surrounding air was lower than that of a full pin, and that this difference enhanced as the ratio of the internal to external diameter grew, perhaps reducing the weight of the heat sink. The performance of the heat transfer was enhanced to 41.6% with the suggested geometry. (Chu *et al*, 2019) have presented a novel triangular heat sink with a different pattern that allows for significant improvements in natural convection. According to CFD simulations that back up this improvement, fin areas measure 150°, 140°, and 2000mm^2 and 3000mm^2, respectively. Heat transfer performance may be greatly enhanced by the triangular fin heat sinks' alternating patterns; increases of up to 14% and 116%, respectively, are possible..

Furthermore, a correlation was suggested to forecast the radial heat sink's average Nusselt number, which may be written as follows:

$$\mathrm{Nu} = 0.195(\mathrm{Ra}^*)^{0.263}\left(\frac{\mathrm{nb_{avg}}}{\mathrm{H}}\right)^{1.35}\left(\frac{\mathrm{r_o}}{\mathrm{L}}\right)^{0.444}\left(\frac{\mathrm{r_o}}{\mathrm{b_{avg}}}\right)^{-0.142}\left(\frac{\mathrm{r_o}}{\mathrm{H}}\right)^{-1.4} \qquad (2.2)$$

Where:

$$\mathrm{Ra}^* = \frac{\rho^2 g \beta C_P \pi (r_o^2 - r_i^2)\dot{q}L^3}{\mu L k^2}$$

$$\mathrm{b_{avg}} = \frac{1}{2}\left\{\left(\frac{2\pi \mathrm{r_o}}{\mathrm{n}} - \mathrm{t}\right) + \left(2\pi\frac{(\mathrm{r_o} - \mathrm{L})}{\mathrm{n}} - \mathrm{t}\right)\right\}$$

The expected values from this equation match the theoretical values with an error percentage of less than 10% and within the following limits:

$$\mathrm{t} = 2\ \mathrm{mm}, 20 \le \mathrm{n} \le 26, 21.3\mathrm{mm} \le \mathrm{H} \le 63.9\mathrm{mm}, 75\mathrm{mm} \le \mathrm{r_o} \le 102\mathrm{mm}$$

$$40\mathrm{mm} \le \mathrm{L} \le 80\mathrm{mm},\ \ 300\mathrm{W/m^2} \le \dot{\mathrm{q}} \le 1100\mathrm{W/m^2}$$

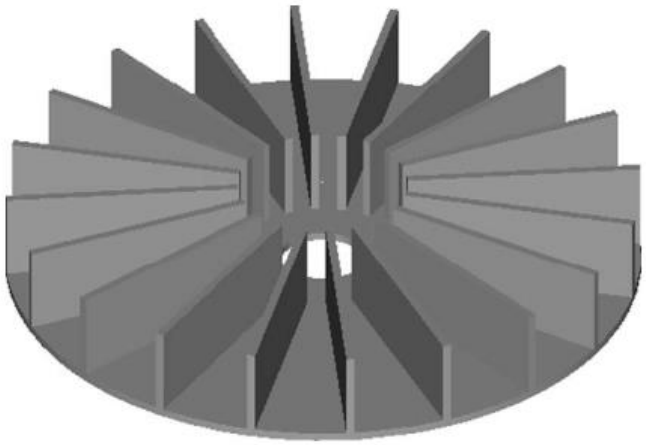

Figure 2.1: The circular base and rectangular fins of the radial heat sink (Hanafi *et al*, 2015).

Figure (2.2) illustrates the configuration of the fins used.

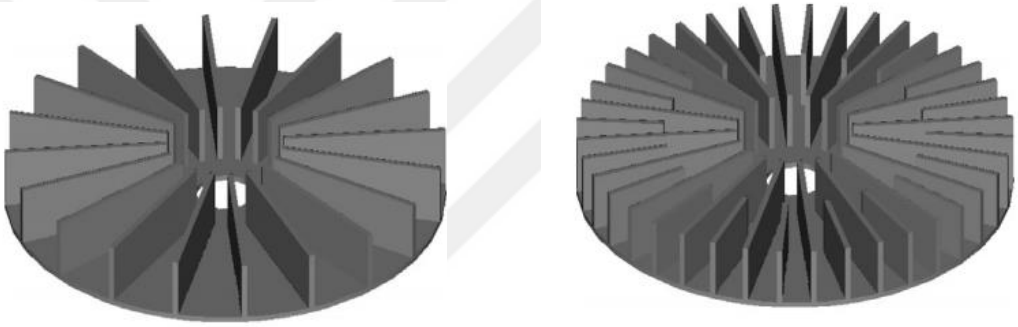

(a) L type model

(b) LM type model

Figure 2.2: Configuration of the fins used in the study (Li *et al*, 2016).

Researchers came up with an ideal radial heat sink design that reduced bulk by over 30% while keeping cooling efficiency close to the finned heat sink (Yu *et al*, 2011). See Figure (2.3).

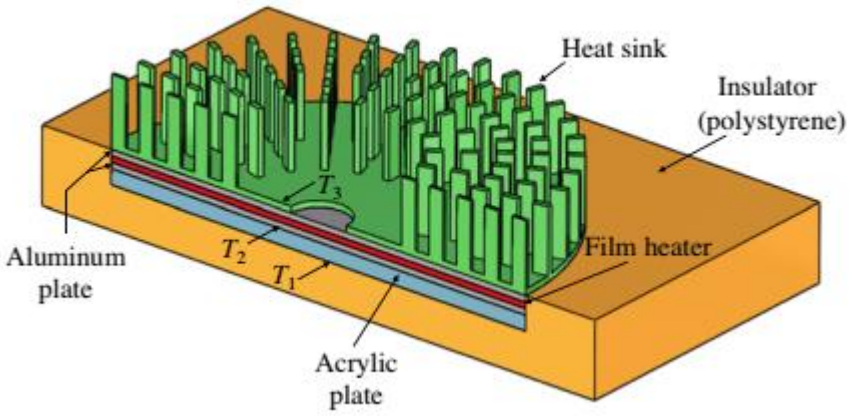

Figure 2.3: Experimental setup diagram of the pin-fin radial heat sink (Jang *et al*, 2012).

(Aziz, 2013) performed a theoretical investigation on the performance of radial fins covered with homogenous and functionally graded material (FGM) under circumstances of free convection and radiative heat transfer. Convective-radiative heat transfer was used at the tip of the fins to cool them, and the fins were all the same thickness throughout. Assuming a linear relationship between temperature and radial coordinates for the homogenous material, the thermal conductivity for the FGM fin was found to be linear. During their theoretical investigation, the researchers employed the Differential Transformation Method (DTM). By displaying accurate temperature variations and fin efficiency, they were able to provide a thorough grasp of fin efficiency under realistic operating settings by comparing the produced model's findings with the precise analytical solution.

In order to enhance the performance of pin-fin radial heat sinks with different heights that are utilized in high power light-emitting diode systems under natural convection and radial heat transfer circumstances, a theoretical and experimental investigation was carried out the following year, in 2014 (Jang *et al*, 2012). The researchers performed experiments to evaluate the theoretical model on different fin height configurations. The results showed that fins with taller heights exhibited better cooling performance compared to other fin configurations. The highest possible fin height and the disparity between the height of the fins and the fin rows number were determined as design criteria. With the same design and mass, the researchers claimed to enhance heat sink cooling efficiency by 50% under combined radiative heat transfer and free convection circumstances. However, under free convection conditions alone, the gain in cooling performance was only about 15%. The researchers came to the

conclusion that, while keeping the same mass as plate-fin heat sinks, the cooling efficiency of pin-fin radial heat sinks with side-fin length variability improved by more than 45% (Li and Byon, 2016 a). For this investigation, a test sample is shown in Figure (2.4).

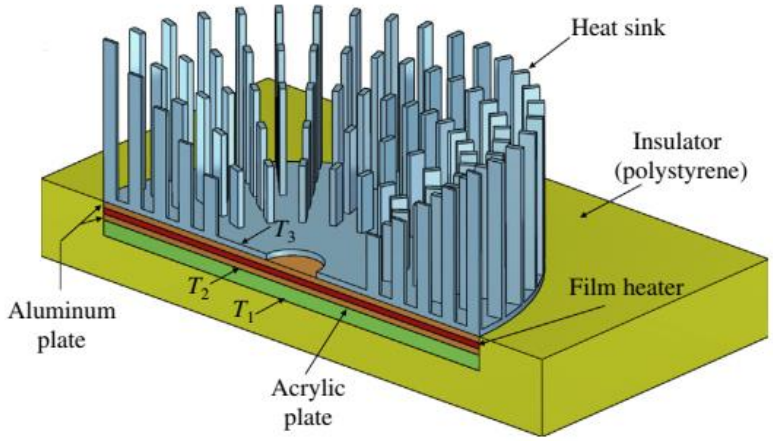

Figure 2.4: Schematic of the experimental setup platform (Li and Byon, 2016 a).

Researchers Li and Byon conducted a theoretical and experimental study in 2015, as mentioned in the source (Li and Byon, 2016 b), to investigate the effect of the orientation of a circular base and concentric annular fins exposed to a free convection heat load. They looked at the effects of orientation angles in relation to gravity and a variety of geometrical factors, such as the base height and the number, length, and height of the fins. They also took into account the non-dimensional number El as a factor influencing the Nusselt number (Nu), which represents the heat transfer coefficient.

The findings demonstrated that while fin length and base height had a very little influence, the number of fins and fin height had a substantial impact. Because of the concentric circular construction that inhibited upward free heat movement, the horizontally waved radial heat sink performed better thermally than the vertically wavy arrangement. The results of the experiment and theoretical findings showed good agreement, with a variation percentage of no more than 0.4%.

In order to forecast the Nusselt number (Nu) according to the heat sink design characteristics, the researchers created a correlation equation.

Researchers (Hanafi *et al*, 2015) provided a theoretical study for the design and enhancement of an example of a radial plane fins heat sink, which is utilized in central processing units (CPUs). The study looked at how the heat sink performed in relation to technical aspects like fin length and thickness. The researchers also sought to determine the optimal layout for this model, one that would maximize heat dissipation while minimizing the size of the CPU's electrical package heat sink. The findings demonstrated that, while utilizing various heat sink kinds and combinations of technical parameters, heat dissipation varied. The researchers also suggested a particle swarm optimization technique for comparing several radial fins and a multi-objective optimization flowchart. The optimal distance for a heat sink with good heat dissipation and small size was allegedly achieved by the researchers.

Researchers (Park *et al*, 2015) described the results of a study they conducted to enhance the structure of a radial heat sink having interwoven fins used to cool light-emitting diode (LED) lights in a technical note that was published in 2015. The scientists created a numerical model and verified it through experiments for multiple pin-fin array heat sinks. Sensitivity analysis was used to determine a set of factors for the design. Using an evolutionary algorithm, a multidisciplinary optimization was carried out based on the heat sink's mass and resistance to heat. The analysis's findings showed that, for a given heat resistance, the radial heat sink with interwoven fins was the best arrangement since it improved thermal performance by up to 10% while keeping mass constant or lowering it by up to 12%. The researchers also said that because this approach resulted in increased performance and safety as well as lower production costs, it was anticipated to offer possibilities for LED bulbs.

Researchers Park *et al*. (2015) have conducted a follow-up study in which they reported a theoretical and experimental inquiry to improve the effectiveness of circular-based radial heat sinks with surrounding structures resembling chimneys that are used to cool high-power light-emitting diode (LED) lights. Long and medium fins were added in the heat sink design. Two numerical models were used: the k-ε model was utilized to analyze the free convective heat load, and the Discrete Transfer Radiation Model (DTRM) was used to analyze the radiative heat transfer from the surrounding structure and heat sink to the ambient environment. The correctness of the model was confirmed by experimentation once the numerical simulation of radiative heat transfer and thermal flow was finished.

By adjusting the airflow pattern within the heat sink, heat transfer by natural convection may be enhanced. This heat sink's small air intake allowed cooling air to reach the center, increasing the airflow velocity surrounding the heat sink as a result of the surrounding construction. The findings showed that adding the surrounding structure resembling a chimney increased the radial heat sink's thermal efficiency by up to 40%. The materials chosen to build the surrounding structure have no bearing on the heat sink's capacity to dissipate heat. It is anticipated that this research will help in the development of naturally cooled high-power LED lighting systems.

The researcher Li and colleagues investigated the heat transfer by natural convection from a perforated radial heat sink in 2016 by conducting a theoretical analysis, as mentioned by (Li *et al*, 2016). The work was documented in a technical note. The number of perforations in the range of 0-6, the diameter of the holes in the range of 0-3 mm, the channel height in the region of 1.5-6 mm, and the angle of inclination in the range of 0 to 180 ° were among the factors that the researchers looked at in relation to the heat sink's ability to dissipate heat.

The findings indicated that the vertically waved radial heat sinks outperformed those waved in other directions in terms of heat dissipation, and that the perforated radial heat sink performed better thermally than the non-perforated version. The study also showed that the geometric features of the perforations greatly influenced the heat dissipation performance of the heat sinks in both the vertical and lateral orientations.

According to the study, the radial heat sink with perforations had a 17% lower thermal resistance than its counterpart without any holes, while the bulk of the perforated structure was lowered by as much as 37%. The unhindered natural heat movement via the perforations may be the cause of this decrease. The heat sink employed in this study is shown in Figure (2.5).

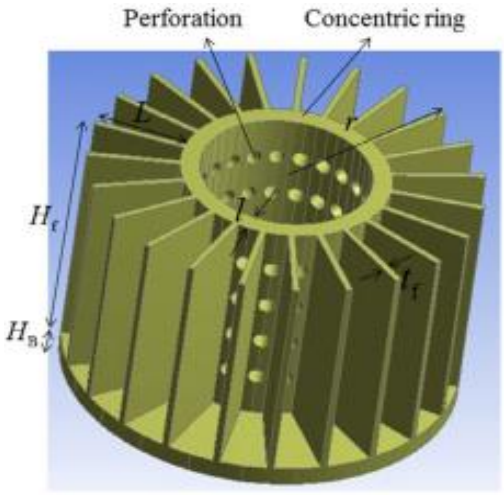

Figure 2.5: Four-perforated radial heat sink (Li *et al*, 2016).

Researchers Li and colleagues (Li *et al*., 2016) provided a theoretical as well as experimental investigation on radial heat sinks based on chimneys operating under free convection circumstances in the same year (2016). A heat sink with and without a chimney was used to compare their respective performances. The inclination angle ($0 \leq \theta \leq 180°$) to take gravity into consideration, the number of fins ($15 \leq N \leq 30$), and the distance ($5mm \leq Hc \leq 25mm$) between the base and the chimney were among the parameters that were examined. The findings demonstrated that the chimney-based heat sink performed best at angles of inclination of 0° and 45°, with worse thermal performance occurring at angles of 135° and 180°. At a 90° inclination angle, the performance was unsatisfactory. The ideal values for Hc and N were also determined by the results. In comparison to a heat sink without a chimney, the researchers asserted that the radial heat sink with a chimney was better and might increase thermal performance by as much as 20%. The results from both experiments and theory showed good agreement, with an error percentage that was no more than 6.5%. Figure (2.6) shows a schematic representation of the model under study.

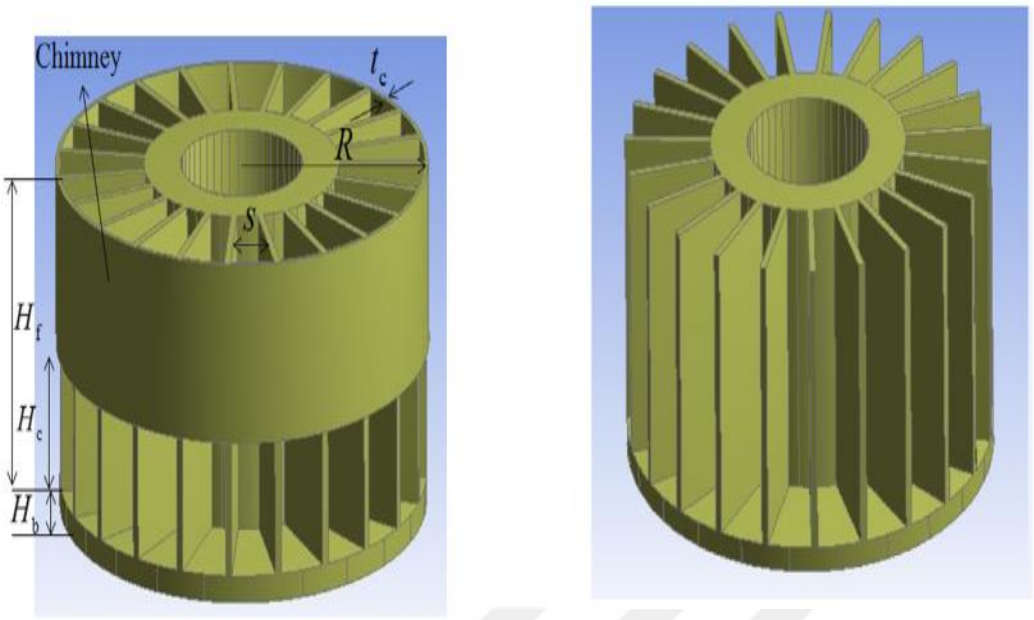

(a) (b)

Figure 2.6: Diagrammatic representation of the heat sink (a) with and (b) without a chimney (Hassan *et al*, 2021).

In 2017, researchers Kwak *et al*. carried out a theoretical and practical investigation on the cooling capabilities of a radial heat sink with triangular fins positioned on a circular base. (Kwak *et al*, 2017). The study was carried out under free convection conditions with different inclination angles. The researchers found that both the Rayleigh number (Ra) and the finning factor, fin density factor, inclination angle, and circular base diameter had an impact on the thermal resistance. They found that both experimental and theoretical research agreed well. To determine the extent of cooling performance improvement, the researchers created a correlation equation.

Kwak *et al*. said that this equation may be used to estimate the thermal resistance of heat sinks for LED illumination, regardless of whether fins are present. The data derived from the equation, with a mean error ratio of under ten percent and a highest error ratio of 11.8%, demonstrated good concordance with numerical results.

Researchers (Kwak *et al*., 2018) carried out a numerical analysis the next year to improve the performance of a radial heat sink that included both convection and radiation heat transfer. The heat sink included a concentric cylinder and triangle fins installed on a circular base. There was considerable agreement between these results and the experimental results when they were compared. The study looked at how many

geometric factors affected the heat transfer coefficient and thermal resistance, including the hollow cylinder's radius, the fin count, the number of fins, and the base radius of the heat sink. Weighted sum method and genetic algorithm were used for multi-objective optimization. In comparison to the conventional radial heat sink, the radial heat sink with triangle fins had less bulk and thermal resistance thanks to the Pareto fronts that were produced. It was discovered by the researchers that it was feasible to lower the heat sink's mass by 10-31% while keeping the thermal resistance constant and by 10-16% while keeping the mass at the same level. The optimization results of this study, according to the researchers, may be helpful in designing of radial heat sinks with triangular fins for LED bulbs applications.

An analytical and experimental investigation was given by (Li *et al*, 2016) in order to enhance the performance of horizontally corrugated radial heat sinks under free convection circumstances. The three fin engineering design parameters—thickness, length, and number—have a broad range of correlations, according to a novel equation that the researchers constructed. They used this correlation to improve the three design parameters for the thermal efficiency of radial heat sinks with perforated fins. As a result, they were able to create an ideal fin design for a variety of application sizes, as the suggested correlation equation can accommodate a range of physical dimensions indicated by fin height and base diameter. This research is useful for engineers working in this field, particularly those designing radial heat sinks with corrugated fins for various applications.

(Hassan *et al*, 2021) experimentally studied heat transfer by the free convection of the radial thermal sink of three and six triangular fins without perforation and circular perforation arranged in a linear and curvy manner to find the thermal performance of this sink and compare these kinds of perforation order. Using three values for the quantity of heat processed: (25.69), (63.58) and (136.96) W, respectively. This study found that many factors affect lowering the temperature including the number of fins, whether fins are perforated or not, the pattern of perforation. According to this study, the heat transmission will increase when there are six fins instead of three. Additionally, the heat transfer coefficient is negatively impacted by fin perforation, particularly when the fins are perforated in a linear pattern.

In order to increase the performance of radially linked plate-fin heat sinks under forced convection heat transfer circumstances, with an L-shaped airflow pattern, researchers (Lee and Kim, 2016) carried out a theoretical and experimental investigation in the same year. Air was pushed to flow from the top and out of the sides of the heat sink, and the heat source was situated at the bottom of the framework, with a similar base diameter as the fins. In order to optimize this heat sink, the researchers created an efficiency equation for the heat sink based on an analytical model and offered an equation for the drop in pressure and average Nusselt number (Nu) based on theoretical data. Several experiments were conducted on the heat sink with different geometries to validate the proposed equations, the results of the experiments and the equations showed a good degree of agreement..

A study by Khan *et al*. (2006) examined the effects of several fin shapes on total thermal/fluid performance, including square, circular, elliptical, and pin fins, as well as rectangular plate fins (Figure 2.7). Nusselt number, Reynolds number, Aspect ratio, and drag coefficient are among the dimensionless variables that are used to formulate the dimensionless entropy production rate. A few selected fin forms' heat transmissions, friction with fluid, and minimum entropy production rate are examined in connection to a variety of variables, including the Reynolds number, axial ratio, and aspect ratio. The results clearly demonstrate the significance of these variables for the intended fin profile.

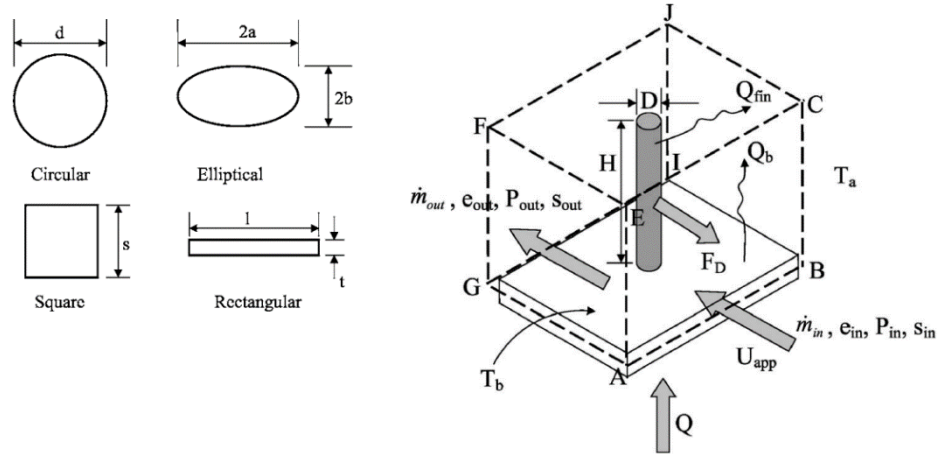

Figure 2.7: Square, circular in shape, elliptical pin fins, and rectangular plate fins (El Ghandouri, 2020).

The researchers came to the conclusion that the best number and fin thickness for the fins under various pumping power situations may be obtained by utilizing these

three correlations: pressure decrease, median Nusselt number, and heat sink efficiency. Lastly, the researchers offered some equations that might be included below as design guidance for radially coupled plate-fin heat sinks (El Ghandouri, 2020).

$$n_{opt} = 1.24\left(\frac{r_r}{H}\right)^{0.3}\left(\frac{L}{H}\right)^{0.3}\left(P^{*}_{pumo}\right)^{0.2} \quad (2.3)$$

$$L_{opt}/L = 0.0878\left(\frac{r_r}{H}\right)^{0.3}\left(\frac{L}{H}\right)^{-0.45}(k^{*})^{-0.4} \quad (2.4)$$

Where:

$$P^{*}_{pumo} = \frac{P_{pump}}{\mu^{3}\rho^{-2}H^{-1}} \quad (2.5)$$

$$k^{*} = \frac{k_s}{k_a} \quad (2.6)$$

Where:

H: is the fin height.

L: is the fin length.

r_r: is the radius of the rigid cylinder.

Researchers (Pua *et al.*, 2019) carried out a theoretical as well as experimental investigation in 2018 to look into the heat transfer via different finned heat sinks used in tiny electronic systems. A mathematical framework was put out, and an experiment was used to confirm its correctness. The heat transfer coefficient was measured experimentally for a bare plate working in both forced and free convection cooling scenarios in sloped vertical and horizontal orientations. Additionally, tests were conducted using free convection cooling on both the cylindrical vertical fin heat sink and the vertical fin heat sink. The objective of the heat sink testing was to keep the operating temperature below 100°C. Additional heat loads that varied from 5 to 40 W were evaluated. The coefficient of heat transfer (*h*) for the following three varieties of finned heat sinks was the main focus of the study:

• Finned heat sinks with bare plates (BP) in vertical, horizontal, and inclined orientations for both forced and free convection cooling.

• Cylindrical fin heat sinks (CFHs), which have a series of rectangular fins oriented radially outward and are vertically inclined while cooling by free convection. A snapshot of both the second and third categories is shown in Figure (2.8).

• Cylindrical fin heat sinks (CFHs) inclined vertically with a set of rectangular fins arranged radially outward under free convection cooling conditions. Figure (2.8) illustrates a photographic image of the second and third types.

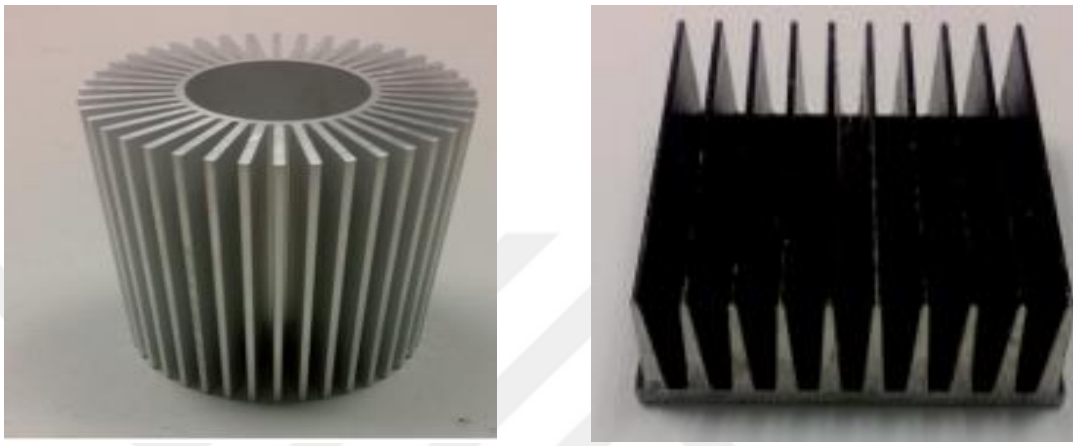

Figure 2.8: A photographic image of the heat sink used in this study (Yildiz and Yüncü, 2004).

The results showed an increase in the heating surface temperature with the added heat as expected. Additionally, the surface temperature was higher when cooling under free convection conditions. At high heat flux, the vertical plate fin heat sinks (BP type) showed lower surface temperatures than the horizontal plate fin heat sinks. When cooled under free convection, the plate fin heat sinks (PFHs) performed better than the other scenarios. Based on the Churchill and Chu equation, the researchers developed the following equation to get the coefficient of heat transfer represented by the Nusselt number (Yildiz and Yüncü, 2004):

$$\mathrm{Nu_L} = 0.68 + \frac{0.670\ \mathrm{Ra_L^{1/4}}}{[1 + (0.492/\mathrm{Pr})^{9/16}]^{4/9}} \quad \mathrm{Ra_L} \leq 10^9 \qquad (2.7)$$

For the majority of the previously described heat sink types under study, the researchers discovered a respectable degree of agreement between the measured values of the heat transfer coefficients and the values calculated from the suggested equations for the Nusselt number.

Researchers studied the free and forced convection heat transfer properties of a radial curved fin heat sink attached to a cylindrical base theoretically and experimentally in 2018 (Khadke and Bohole, 2018). The fin height, fin spacing, and heat input rate were the geometric characteristics under investigation. When the airflow velocity was changed, a temperature decrease was noted while maintaining a consistent heat input rate. To get the heat sink's Nusselt number (Nu), the non-dimensional fin height fell between $0 \leq Z^* \leq 1$ and the number of fins between $0.4 \leq El \leq 2.8$. The findings indicated that there was less of a temperature differential between the fin's top and bottom halves. As a result, the outer surface had a greater heat transfer coefficient and Nusselt number. Between this work and earlier research, the researchers discovered strong agreement.

Researchers (Sundar *et al*., 2019) conducted an experimental and theoretical study in 2019 to examine the efficiency of a radial heat sink with short, staggered fins that are both perforated and non-perforated under circumstances of radiative and free convection heat transfer. A picture of the heat sink employed in this investigation is seen in Figure (2.9). The fin factor, permeability factor, and alignment angle were taken into account by the numerical model in order to improve heat transfer efficiency and lower heat sink mass. Analytical calculations were performed using the permeability factor, fin factor, orientation angle, base radius, and heat flow to calculate the thermal resistance for both scenarios. The theoretical and experimental findings agreed well, with an error rate of no more than 10%. In comparison to a heat sink without perforated fins, the staggered arrangement of the heat sink performance lowered the thermal resistance by around 7% to 12% in various orientations, and also decreased the bulk of the heat sink by roughly 9%. The researchers also observed that the orientation angle had very little effect on the perforated heat sink's thermal resistance. Because it improved heat transmission capabilities and decreased heat sink mass, the researchers suggested utilizing this suggested arrangement to improve the efficiency of LED lighting fixtures.

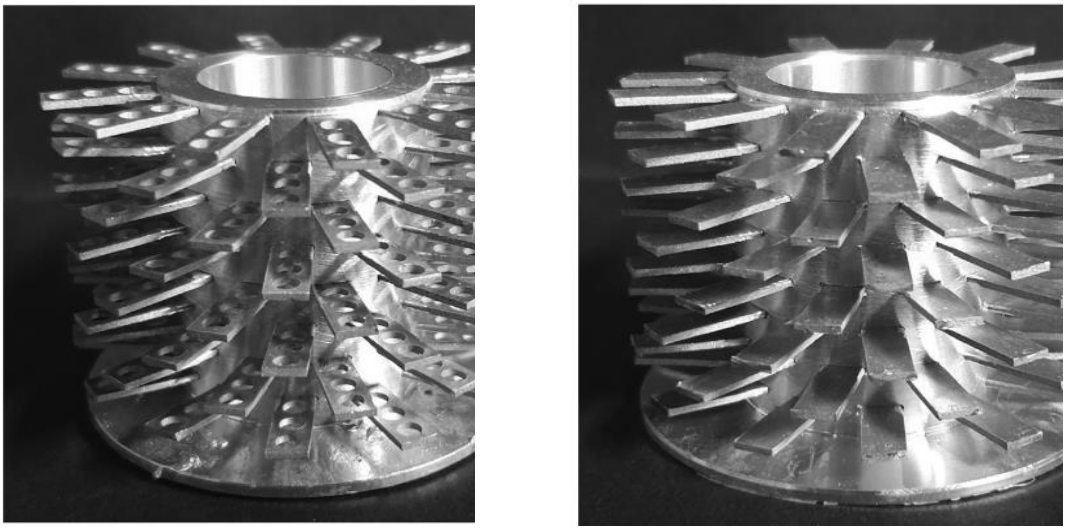

(a) (b)

Figure 2.9:Photographic images of the heat sink (a) perforated fins, (b) non-perforated fins.

A "rippling" fin shape has been developed by (El Ghandouri *et al*., 2020) that may be formed from rectangular flat plate fins fastened to a flat plate. They found that the mass effective heat transfer coefficient increased by 100% and the base plate's temperature dropped by up to 20 °C when oriented vertically. Conversely, the fins of a cylinder can either be longitudinal or annular. For horizontal cylinders, annular fins are more effective in facilitating natural convection, but for vertical cylinders, longitudinal fins are more effective (Yildiz and Yüncü, 2004; Hahne and Zhu, 1994). (Haldar, 2004; Haldar *et al*, 2007) have conducted a study on longitudinal fins attached to horizontal cylinders and the utilization of extra fins with a small height in relation to the surface area. Regarding longitudinal fins on vertical cylinders, there exist a limited number of such instances. (Prakash and Patankar, 1981) have conducted an investigation on vertically oriented tubes with internal fins. (Kumar, 1997) has studied convection occurring naturally within a vertical annulus including longitudinal fins. (An *et al*, 2012) have conducted an experimental study on the heat transfer by natural convection in vertical cylinders with longitudinally installed fins, and they have provided a correlation for these heat sinks with an error of less than 20%.

Researcher have provided significant contributions to the creation of complex fin-structured heat sinks that operate on natural convection. heat sinks with longitudinal fins that are hollow and vertical cylinder heat sinks created by (Shen *et al*, 2016). (Costa

and Lopes, 2014) conducted research to determine the ideal fin arrangement for a radial plate-fin heat sink using numerical simulations. It was possible to determine how sensitive the thermal performance was to changes in design parameters like fin thickness, fin number, and fin length using CFD analysis. Until the required thermal performance was attained, the structural parameter with the highest sensitivity was mostly chosen from the prior fin geometry. This process was repeated. Due to the requirement to numerically evaluate the thermal performance of each fin configuration, their optimization method can be computationally and time-consuming. Furthermore, to get the optimal shape for further applications, an other series of calculations has to be performed.

By using both experimental and numerical techniques, (Yu *et al*, 2012) investigated heat transfer in radial heat sinks by considering radiation and natural convection into considerations. They used three radial heat sinks with varying emissivity evaluations for their investigations. They establish that, given a range of emissivity values, the radiation contribution to the total heat transfer is 27%. By considering radiation heat transfer into thought, (Feng *et al*, 2018) have investigated a novel cross-finned heat sink design that enhanced heat transmission through natural convection with a comparatively simple construction. Their paper claims that the recently created cross-fin heat sink provides a good substitute for traditional plate-fin heat sinks. In their research, they conducted experiments. (Noda *et al*, 2005) established the ideal arrangement for an L-shaped-operating radial plate fin heat sink (RPFHS). Four RPFHS prototypes were created, all of which had the same box size but varied in the amount of fins. To reduce thermal resistance, they chose the ideal heat sink shape, out of the four PFHSs. Even though numerical and experimental approaches are frequently utilized for optimizations', determining an ideal geometry frequently involves laborious laboratory work and large-scale computer computations. Conversely, if accessible, analytical techniques based on closed-form correlations might be helpful in identifying the ideal geometry at a minimal cost and effort. As far as the author is aware, no connection involving PFHSs has been suggested. (Iyengar and Bar-Cohen, 1998) have used a method known as least-material optimization to study the heat sinks' thermal efficiency when fitted with plate fins, triangle fins, or pin fins oriented vertically and fixed to a rectangular base, with an emphasis on natural convection. Finally, they concluded that, under particular conditions, a heat sink with triangle fins

proved to be more thermally efficient than heat sinks with pin and plate fins. (Al-Jamal and Khashashneh, 1998) conducted an empirical investigation to look at the impacts of triangular fins and pins connected to a rectangle foundation in a constant heat flux environment. As opposed to triangular fins, pin fins produced a higher Nusselt number, according to the experimental results, which showed a positive correlation between the two parameters.

In many aspects, the design of heat sinks has changed recently, and these changes have implications for turbine engines, microelectronic chips, and aerospace vehicles (Li and Yang, 2023). According to (Muneeshwaran *et al*, 2023), air did not penetrate farther into the channels than the sideward region of the natural convective heat sinks. Actually, the bulk of the air did not actively contribute to heat transfer since it reached the straight fins heat sink from its sideway area instead of the heat sink itself. Consequently, its ability to improve heat transfer efficiency by the straightforward adjustment of fin dimensions and orientations was limited. As shown in Figure (2.10), they concentrated their study on fin length and fin spacing and proposed a novel inward-notch fin design with a piece of fins cut in the heat sink's center to increase air circulation into the plate heat sink.

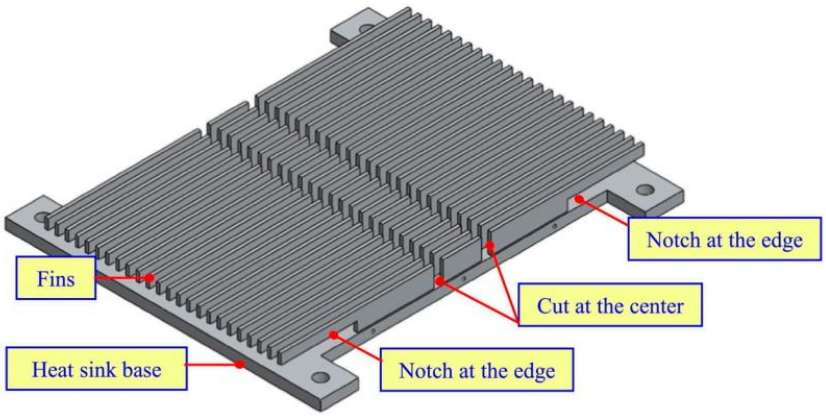

Figure 2.10: The application of notched fins in heat dissipation.

As seen in Figure (2.11), (Rao and Somkuwar, 2021) proposed a tapering fin form to reduce thermal resistance and maximize heat transmission. They examined 1◦, 2◦, and 3◦ tapered angles. They used a power range of 5 to 80 W to heat the heat sink's base in their experiment. The results showed that a broader tapered angle had no positive effect on heat dissipation because of the air retention at the fins origin. The

tapered fin heat sink's overall heat transfer coefficient increased significantly in comparison to the conventional straight fins.

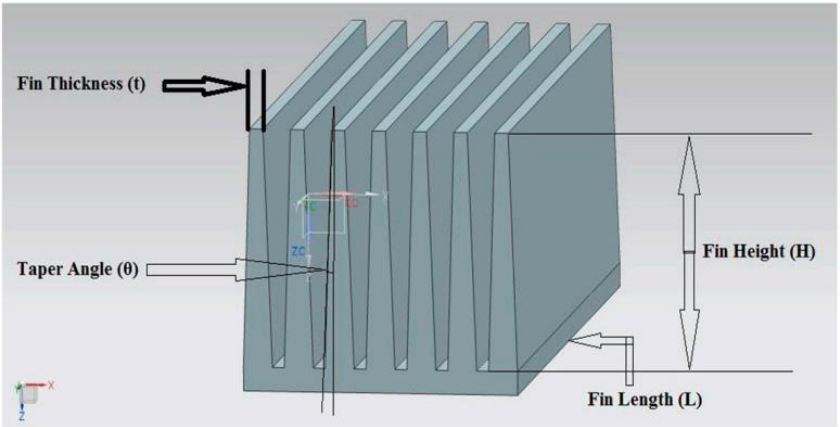

Figure 2.11: The use of tapered fin shape to increase maximum heat transfer by (Rao and Somkuwar, 2021).

Huang *et al*. (Huang and Chen, 2022) changed the relative positions of the fins that were attached to the heat sink in order to replicate the thermal layer of boundary between the fins. Their research was novel and distinctive because it combined previous heat-dissipation techniques with straight-fin heat sinks used in natural convection situations, where the height of the fins and the change in displacement were simultaneously considered as design parameters. Based on numerical results, fin displacement was shown to be more significant than fin height when comparing three straight-fin heat sink designs, including the creative form seen in Figure (2.12).

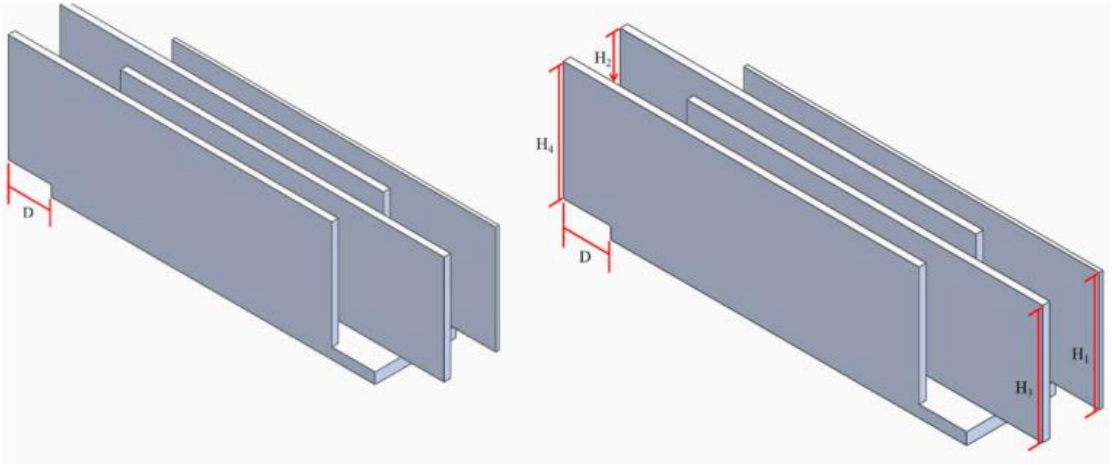

Figure 2.12: Utilizing thermal boundary layers between the fins by (Huang and Chen, 2022).

To increase the heat transfer capacity of a natural convection heat sink, (Feng *et al*., 2018) designed a cross-fin heat sink with a sequence of both short and long fins oriented perpendicularly, as shown in Figure (2.13). Numerical models accounting for natural convection and heat radiation were validated by experiments. When it was shown that cold air could enter every short-fin channel and create an impinging-like flow towards the channel end walls, the cross-fin heat sink performed superior in terms of heat transfer improvement.

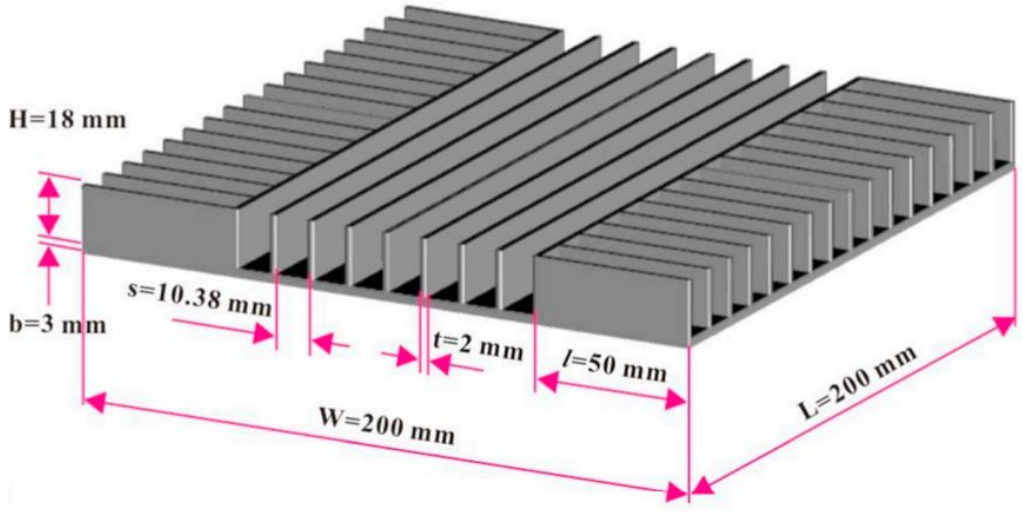

Figure 2.13: The cross-fin heat sink design by (Feng *et al*, 2018).

Following recent developments in additive printing, researchers have begun examining complex geometries such as the "triply periodic minimum surface (TPMS)" cellular framework and the branching fin structure, which were previously

challenging to produce using traditional manufacturing techniques. (Baobaid *et al*, 2022) looked at an optimization problem both experimentally and numerically. As seen in Figure (2.14), they created a heat sink with a Y-shaped shift for natural convection. Their work aimed to decrease base surface temperature and improve cooling effectiveness by designing the fin parameters (for example, the optimal branching angle, shift distance, fin stem height, and fin branch length) under certain circumstances. These results validated the optimized geometry of the Y-shaped-shifted heat sink.

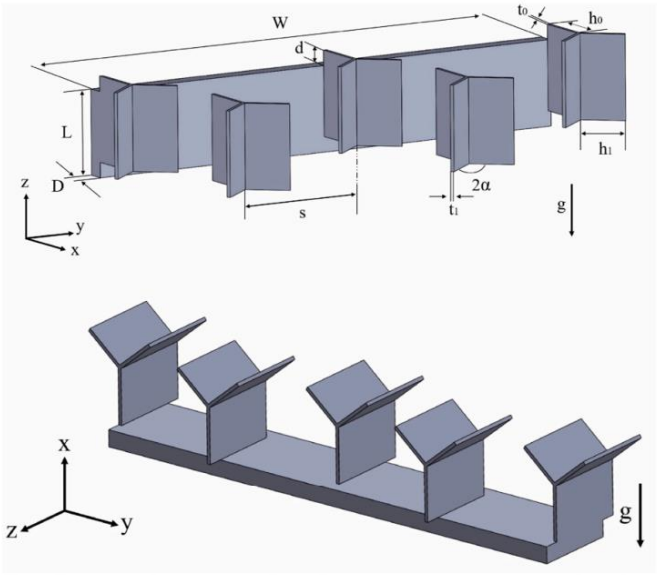

Figure 2.14: The Y-shaped heat sink by Huang *et al*.

(Baobaid *et al*., 2022) examined three separate kinds of heat sinks with TPMS bases: diamond-solid, gyroid-solid, and gyroid-sheet, as shown in Figure (2.15). The experiment was carried out in a natural convection setting with several types of enclosures. In the same experiment, they found that TPMS heat sinks have greater effective thermal conductivity due to a 35–50% increase in thermal efficiency when compared to a typical pin-fin heat sink. The air temperature is often taken to represent the average temperature of the atmosphere, and natural convection has a low coefficient of heat transfer. Therefore, the experiment's setup utilizing the aforementioned guidelines employed a source of heating power of less than 80 W to avoid overheating electrical components. These experiments had a median coefficient of heat transfer less than 15 (W/m^2. K).

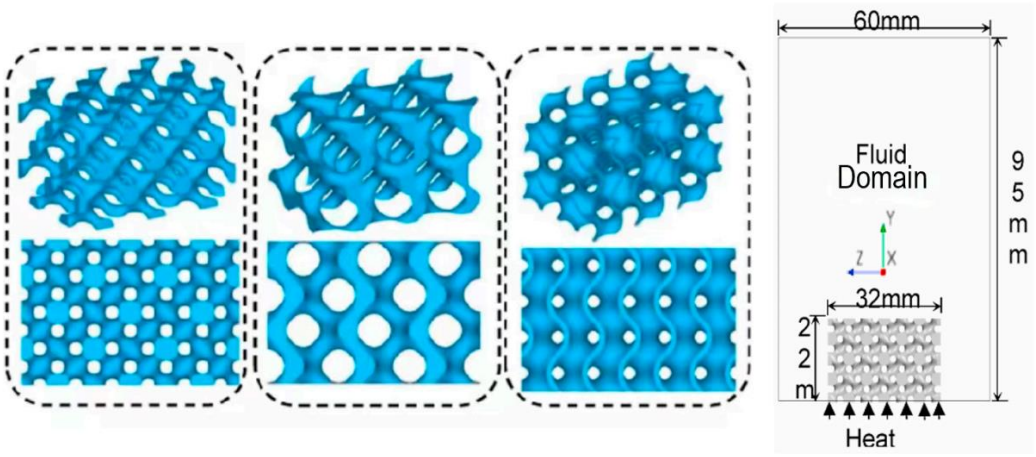

Figure 2.15: The three designed types of heat sinks with TPMS bases by (Baobaid *et al*, 2022).

2.3. Subject of The Current Study

After reviewing the latest research literature on radial heat sinks, it was observed that there are few studies in this area, and they are relatively rare, especially when the fin shape is double triangular. Due to the significant and recent applications of these heat sinks, particularly in modern LED lamps, it was necessary to conduct such a study to assess the benefits of using such fin configurations. The goal of the current study is to ascertain the benefits of such configurations through experimental work on twin triangular fin radial heat sinks having adjustable fin waist. It is important to note that the current study is carried out in a free convection heat transfer environment.

3. MATERIAL AND METHOD

3.1. Introduction

This chapter includes the specific details of this study regarding the preparation for setting up the experimental test facility, measurement devices, and the manufacturing materials for this setup. Additionally, it involves the necessary strategies to conduct the tests specified by this study. This is accomplished by developing a systematic operational plan for conducting the required tests in a sequential manner. Planning ahead for all experimental conditions, including controls, and thinking about all of the materials needed is essential for the smooth running of the experiment. Physical model test planning is an ongoing activity that necessitates a thorough comprehension of the procedures to be mimicked and the methodologies used. Text Figure (3.1) provides a road map to help plan an experimental program, including preparing a list of all the things to accomplish and identifying the important dependent variables to be measured.

3.2. Current Research Strategy

Figure (3.1) exhibits a block diagram of the current research methodology's strategy frame. Once the research vision is established, preparations are made the research component, which involves setting up the experimental facility by procuring the necessary materials, equipment, and tools, followed by arranging and preparing the experimental work cases and their conditions. After completing the required readings through the predefined cases, the collected experimental data. Once this stage is completed, the collected data is analyzed, and calculations are performed, which are then presented graphically, such as in the form of curves or tables. Finally, the conclusions and suggestions for further study provide a summary of the framework strategy's results.

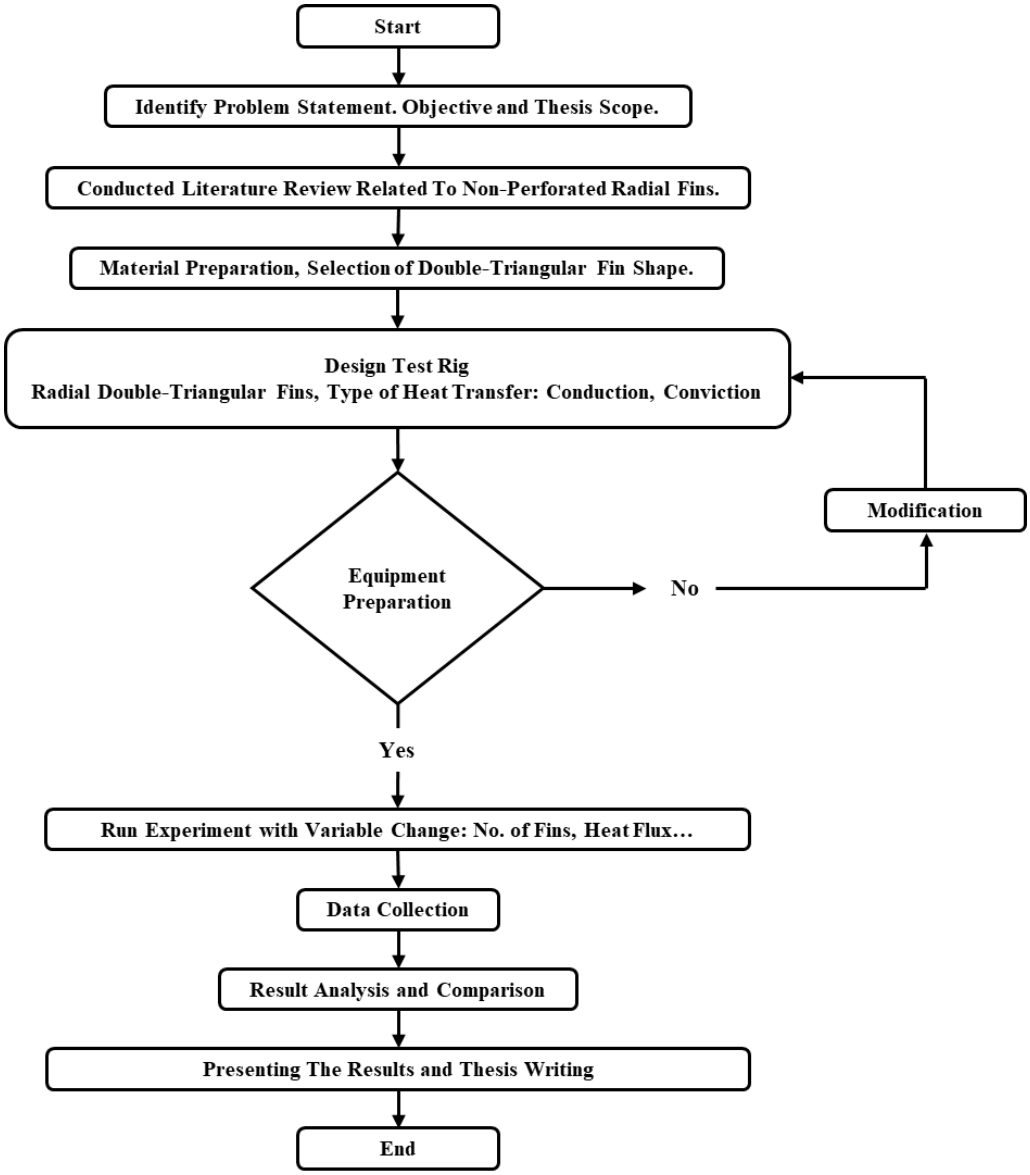

Scheme 3.1: The strategy and methodology for the current research.

3.3. Experimental Setup

In the current experimental study, the heat transfer process will be calculated and measured, resulting in the generation of thermal power in the electric heater due to the flow of electrical current. This heat will then be transferred through three methods: one by radiation, another by conduction, and the last by natural convection. The main factors involved in this heat transfer process require calculations related to the nature of heat transfer, Nusselt number, Rayleigh number, heat transfer coefficient, and the fin efficiency and performance.

A detailed description of these components and equipment is provided in the subsequent sections.

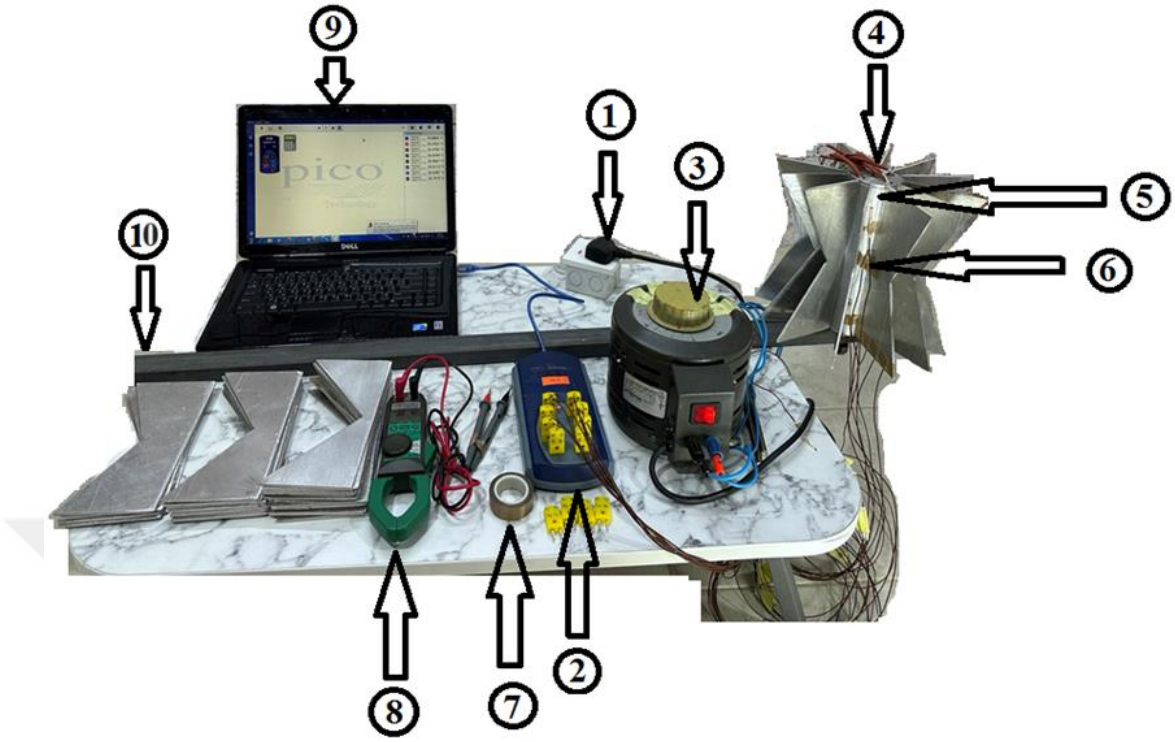

Figure 3.1: System setup.

The following elements make up the experimental setup shown in Figure (3.1) in photography and Figure (3.2) in schematic diagram form:

No.	Part Name	No.	Part Name	No.	Part Name
1	Electrical port	**4**	Cartridge heater	**7**	Tape
2	Data logger	**5**	Test rig	**8**	Voltage and current measu.
3	Power supply	**6**	Thermocouples	**9**	Labtop
10	Steel Arm				

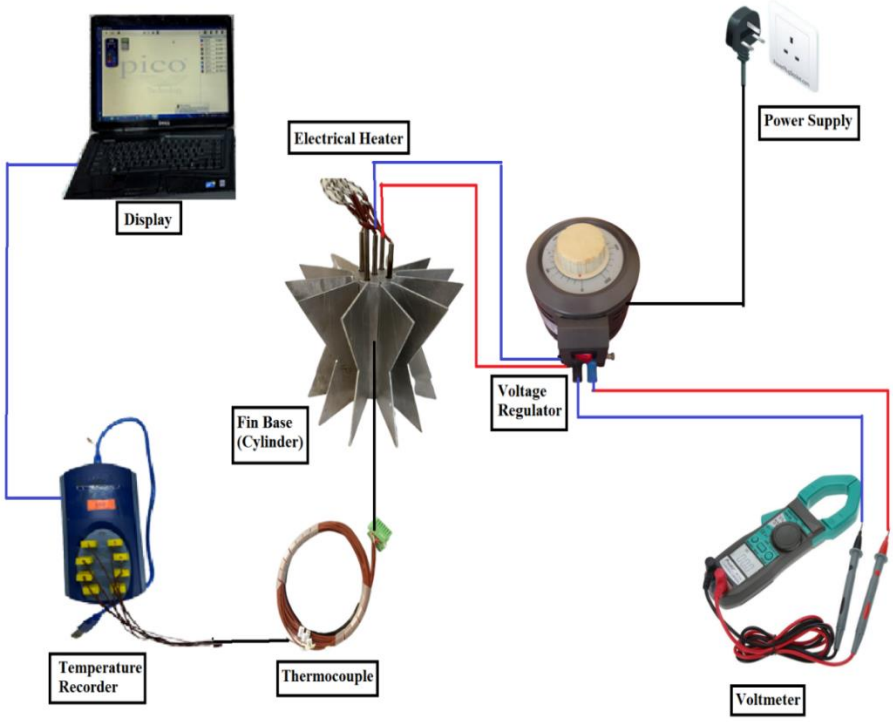

Figure 3.2: Illustration depicting the configuration of the experimental arrangement.

3.4. Materials

The description of the system parts and equipment is detailed as follows:

3.4.1. Cylinder (Fin Base)

The configuration comprises a cylindrical base made of solid metal, measuring 70 mm in diameter and 210 mm in length. On the upper side of the cylinder, five holes were made, each with a diameter of 8 mm and a depth of 200 mm, as shown in Figures (3.3).

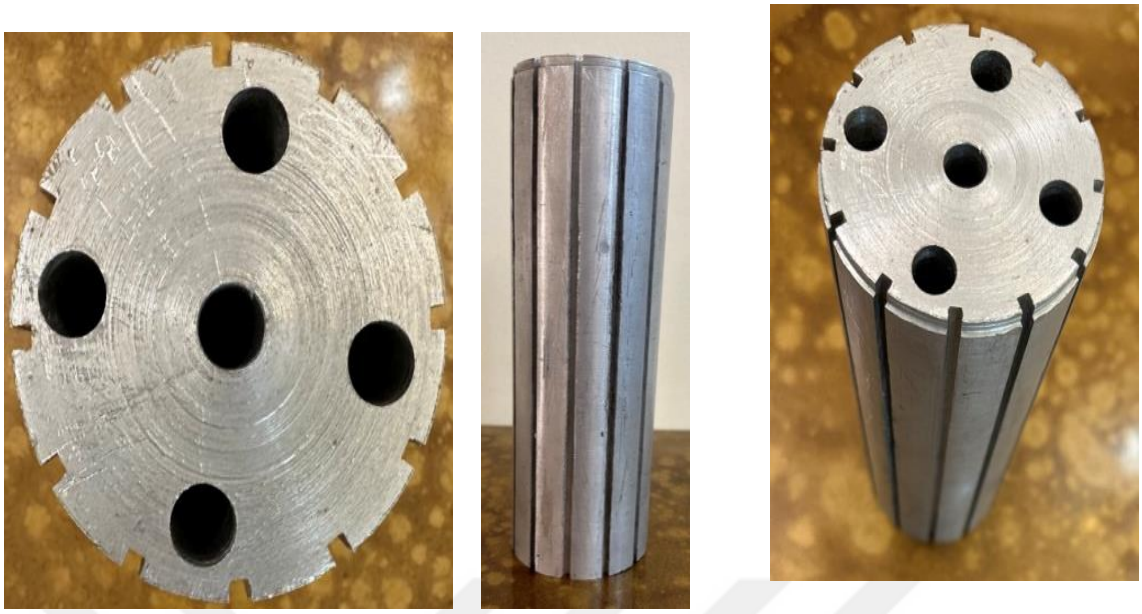

Figure 3.3: Photographs of the cylinder with drilled holes.

Figure (3.4) presents a schematic representation of the cylinder, including its dimensions.. The drilling process was performed on the top cylinder base (fin base) after determining the center of the cylinder (R = 35 mm) to create the first hole. Then, the remaining four holes were positioned by measuring a distance of 17.5 mm from the cylinder center with a 30^{o} angle between them. These holes were designed to accommodate electric heaters, as shown in Figure (3.5). Additionally, twelve longitudinal slots were created with the fins are affixed to the external surface of the cylinder, measuring 3 mm thickness, 3 mm depth, and 210 mm length. The angle between each adjacent slot was 30^{o}.

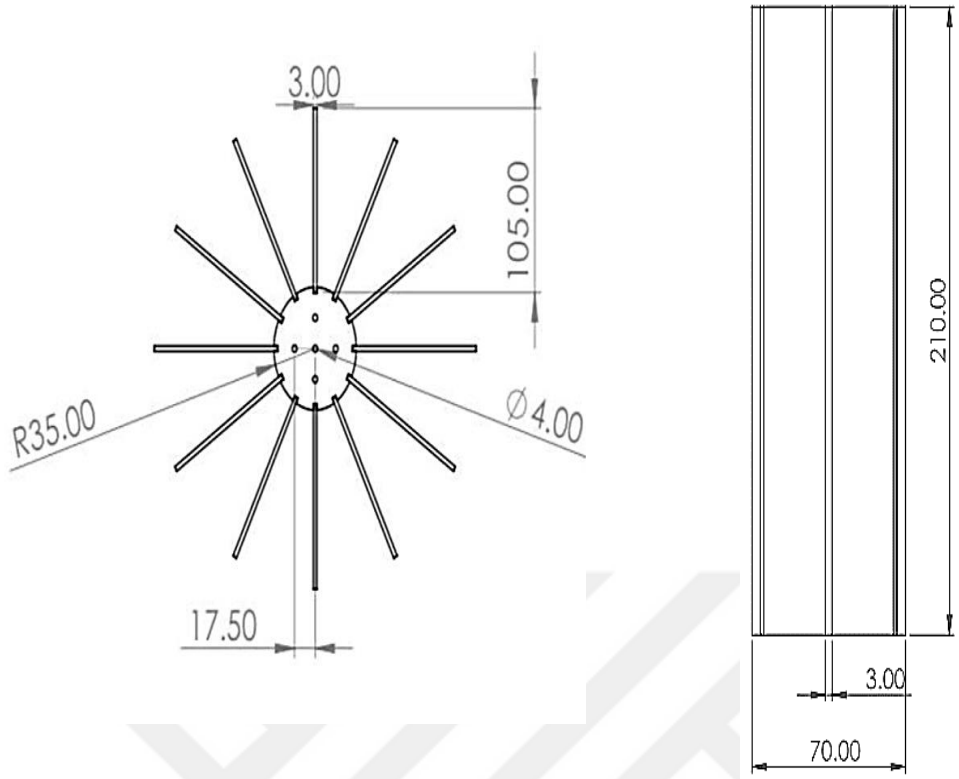

Figure 3.4: Cylinder base schematic illustration with dimensions specified in millimeters.

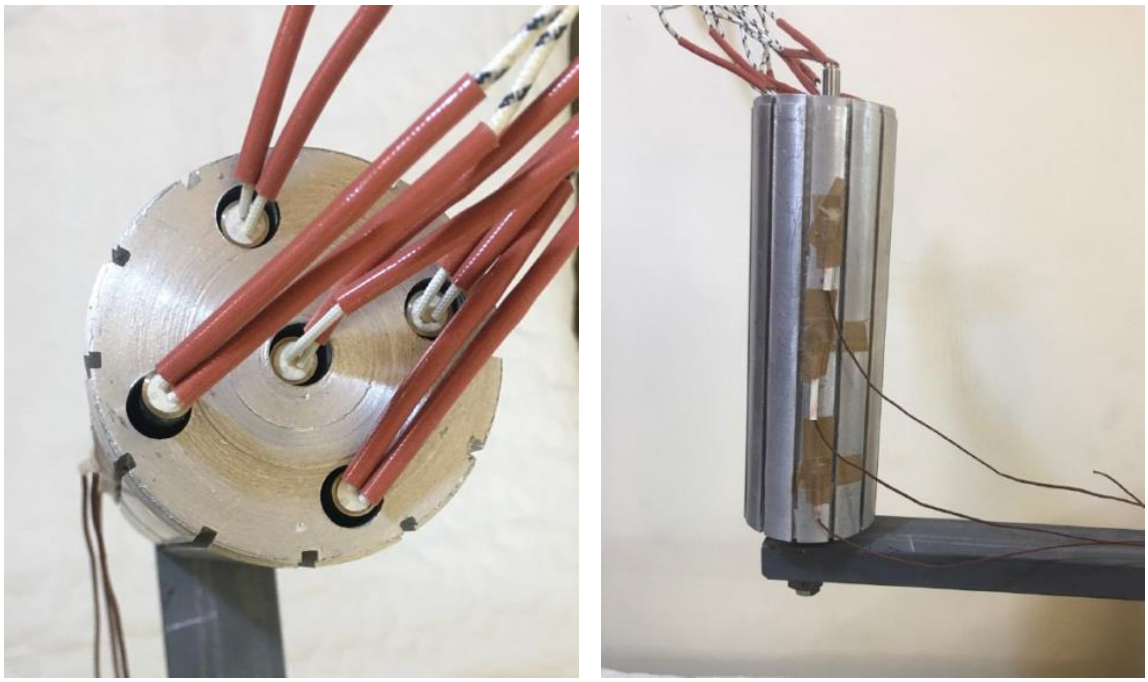

Figure 3.5: Photographs of the base cylinder with thermocouples fixed and electric heaters assembly.

3.4.2. Fins

In this study, three cases of double triangular fins were considered: fins with shafting in the mid of length are 15 mm, 35 mm, and 55 mm. The base cylinder length is 210 mm, and the aluminum fins have a thickness of 3 mm. The right-angled triangle form measured 105 mm at its base, as depicted in the Figures (3.6) to (3.8). The schematic diagram of the installation fins on the cylinder surface show in Figure (3.8). A total of 36 models of triangular fins were manufactured with different shapes, including 12 triangular fins with a 15 mm taper, 12 triangular fins with a 35 mm taper, and 12 other fins with a 55 mm taper. Figure (3.9) show schematic diagrams of the fins with dimensions.

Figure 3.6: The 3D design of the selected fins.

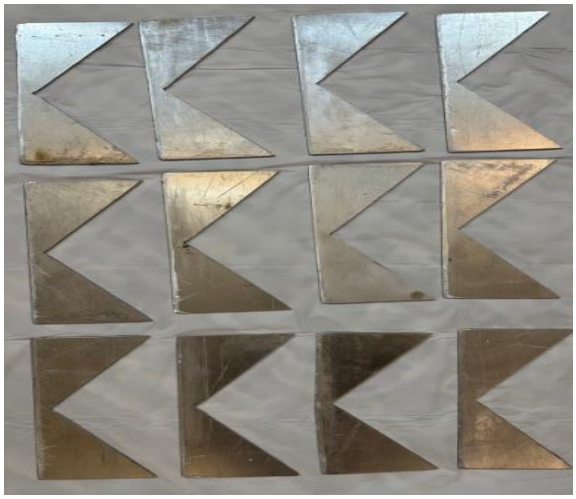

(a)

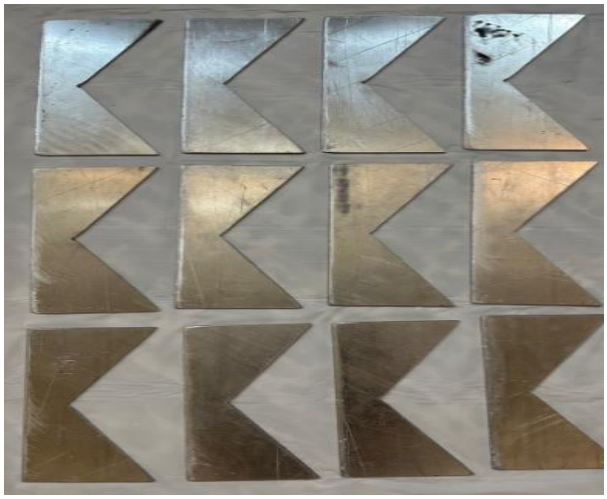

(b)

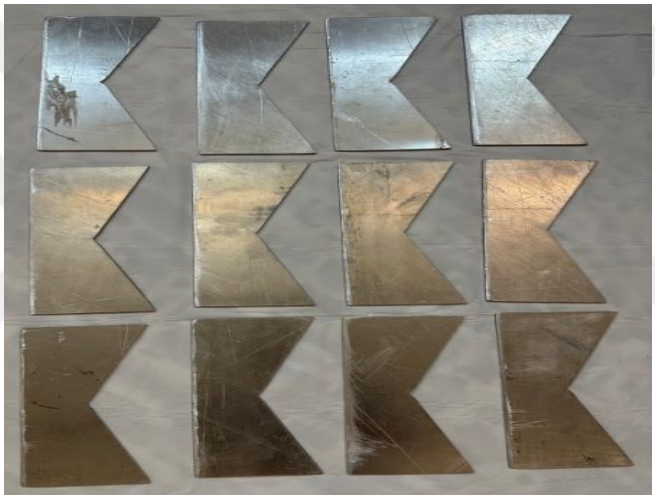

(c)

Figure 3.7: Photographs of the fins used in this study. (a) The fin with drop 15 mm in the middle. (b) The fin with drop 35 mm in the middle. (c) The fin with drop 55 mm in the middle.

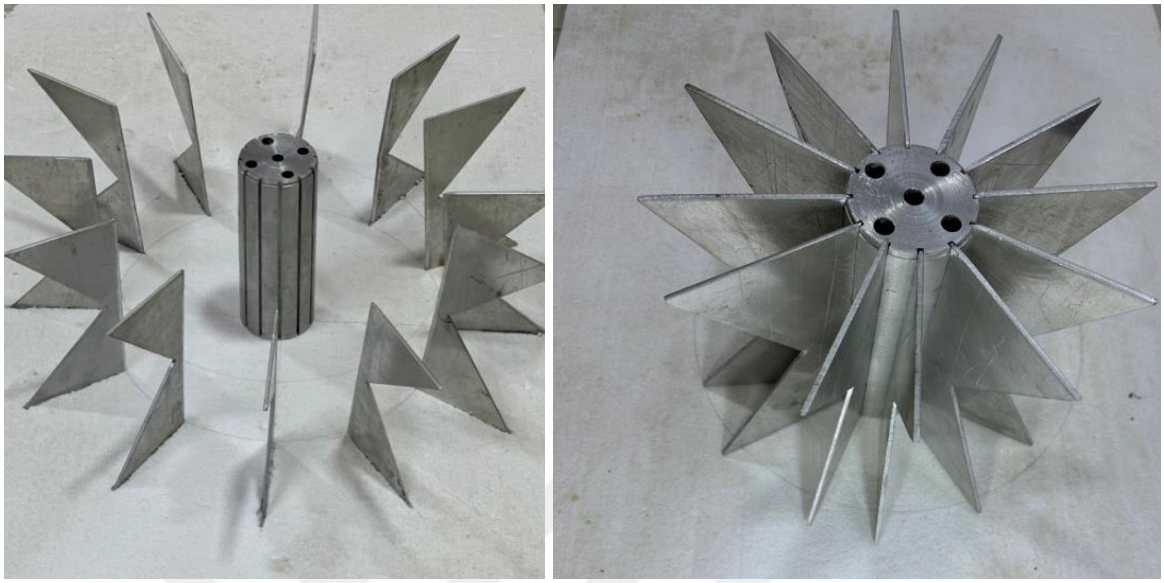

Fins (before installation) Fins (after installation)

Figure 3.8: Schematic diagram of fins installation on the cylinder surface.

Figure (3.8) shows the fin installation required for testing in terms of shape and number on the base of the fin (Cylinder) by inserting it into the pre-existing incision using a flexible plastic hammer to maintain the design of origin (cylinder, fins) without damage.

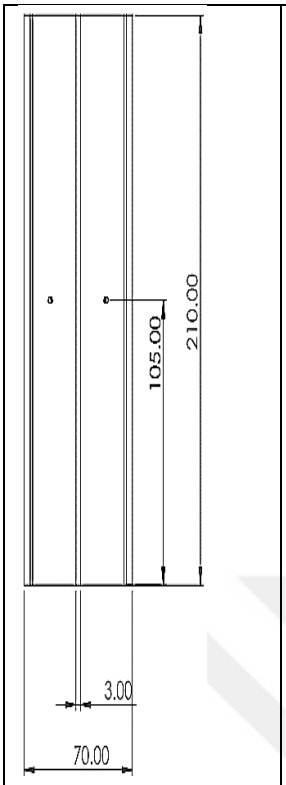

Fin Base Cylinder

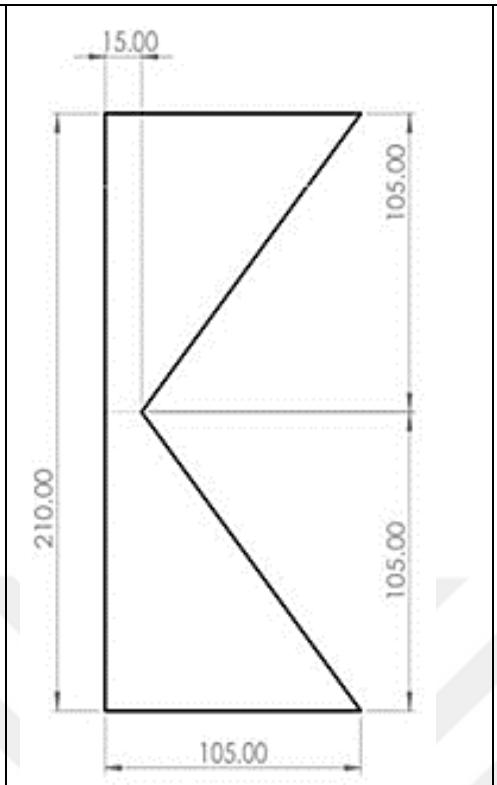

Fin dimensions

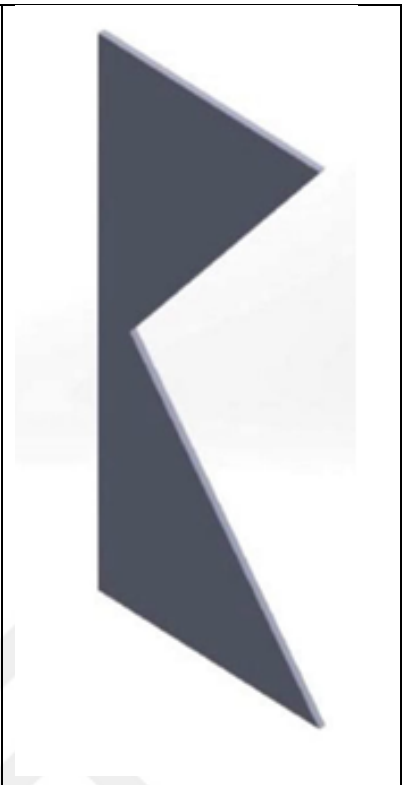

Side-view of the Fin

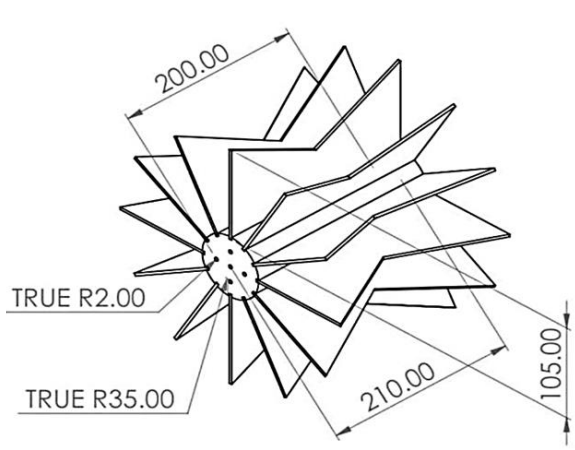

Schematic figure of the system

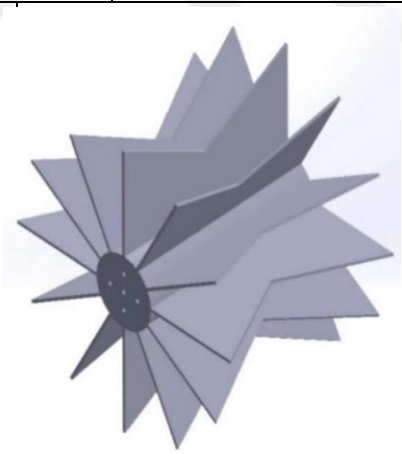

3D view of the system

Figure 3. ***3.9***: Three-dimensional diagram of fins after being attached to the cylinder base with their dimensions.

3.4.3. Temperature Measurements

The Pico Technology USB TC-08 data acquisition model for thermocouple data loggers includes an industrial temperature recorder metre with eight channels and an LCD display (see Figure 3.10). The data logger has an accuracy of 0.2%±1°C and a

measurement range from -200 °C to 1300 °C. The interface is depicted in Figure (3.11) below.

Figure 3.10: TC-08 program interface.

3.4.4. Voltage Regulator

The HSN 0103 220V PLUG To control how much electricity was supplied to the electric heater, a single-phase voltage regulator was used. This voltage regulator allows for adjusting the output voltage within the range of (0 to 250 volts), there by controlling the value of heat flux supplied to the base cylinder (see Figure 3.11).

Figure 3.11: Voltage Regulator Device.

3.4.5. Electrical Heaters

Five cylindrical electric heaters (Cartridge heaters) were used with 8 mm diameter and 200 mm length. Their power dissipation range spans from 50 to 850 watts when operating at 220 volts, as shown in Figure (3.12).

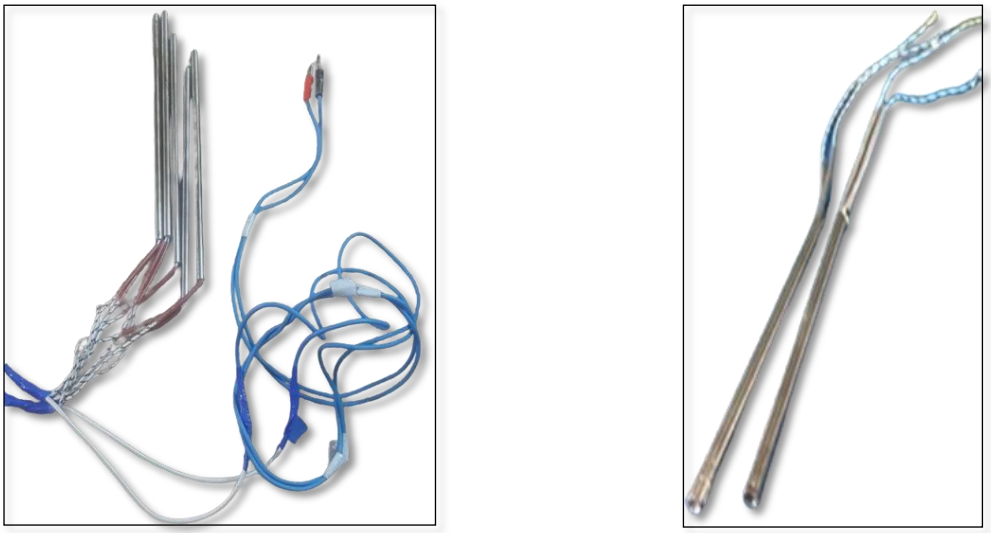

Figure 3.12: Cartridge heaters using in this study.

3.4.6. Electric Current and Voltage Measurement

A multi-meter device, specifically the Pro'sKit MT-3102 clamp meter model, was utilized to assess the voltage difference and electric current flowing from the power supply to the electric heaters. The accuracy of voltage measurement for the range (200-2V) is (1.2%±5), while for current measurement within the range (20-0.4A) it is (3%±15), (see Figure 3.13).

Figure 3.13: Multi-meter device for voltage and current readings.

3.4.7. Thermocouple

Temperature is quantified with eight precisely calibrated K-type thermocouples. Four of the aforementioned thermocouples are attached to the fin wall, whilst three are situated at the base of the cylinder. An independent K-type thermocouple is utilized to gauge the surrounding temperature external to the heat sink. (Figure 3.14). The base temperature of these thermocouples was almost uniform in the vertical direction, Thermocouple locations are shown in Figure (3.15). Furthermore, they were capable of measuring temperatures with a maximum difference of less than 0.3 ℃. Temperature data was gathered using a multi-channel data collecting system.

Figure 3.14: Thermocouple Type K used in the experimental work.

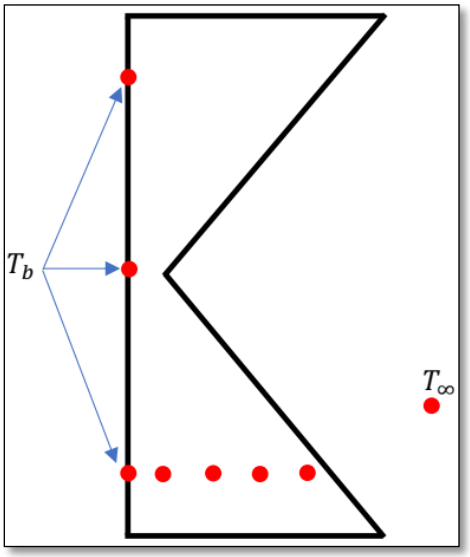

Figure 3.15: Thermocouples locations.

3.5. Thermocouple Calibration

The thermocouples were calibrated with a mercury thermometer under three different conditions: the first reading was taken inside the laboratory, the second reading was taken outdoors in a shaded zone, and the final reading was taken by exposing the thermocouples and the mercury thermometer to sunlight zone. The readings were used to plot a relationship and determine the error percentage in the thermocouple readings, as shown in Figure (3.16). Based on this, Eq. (3.1) was corrected reading of the thermocouples.

$$T_{\text{Thermocouple}} = 1.041 \times T_{\text{Thermometer}} - 0.351 \qquad (3.1)$$

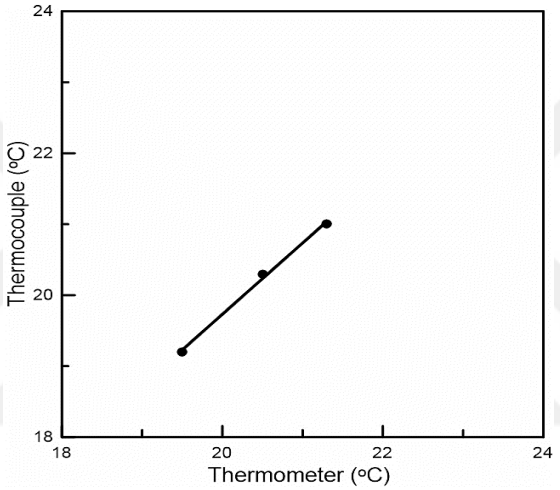

Figure 3.16: Thermocouple calibration.

3.6. Methods

3.6.1. Components of The System

The test apparatus is a round, solid aluminum metal cylinder that is 70 mm in diameter and 210 mm in length. Along the length of the cylinder, five impermeable holes were drilled with a diameter of 8 mm and a depth of 200 mm on the upper surface. The perforation process was completed for the fin base cylinder's upper surface following the cylinder's center was determined (R=35mm) to drill the first hole, and then the other four holes were determined by specifying a distance (17.5 mm) from the center of the cylinder and at an angle (30°) to be placed Electric heaters are inside these holes. To install the fins along the cylinder's outside, twelve longitudinal incisions that formed a channel with a thickness of three millimeters has been created, a depth of three millimeters, and a length of 210 millimeters, noting that the angle between one incision

and another was 60°. Table (3.1) and Figure (3.17) presented the cases in this study. Use a 24-channel Applent Multi-channel Temperature Meter AT 4524, which uses several types of thermocouples. The accuracy of the device is (0.2% + 1℃) and the range of readings is (-200) to (1300). In this research, nine locations were installed to measure the temperature, six of which were on one of the fins in different locations, and two were on the body of the cylinder, from which the average was taken, which is considered the surface temperature of the cylinder, and the other location was for the air surrounding the test platform.

Five rates of additional heat (20.16, 66.03, 105.30, 157.62, and 196.08 Watt) were investigated in this study. Based on physical criteria such fin height, length, and distance between fins, as well as the influence of the flowing heat rate, represented by the Raleigh number, a relationship was constructed to determine the Nusselt number.

3.6.2. Test Preparation Procedure

Before each test the following steps are followed and for all three fin cases I, II, and III:

1. Fin installation required for testing in terms of shape and number on the base of the fin (Cylinder) by inserting it into the pre-existing incision using a flexible plastic hammer to maintain the design of origin (cylinder, fins) without damage.
2. Inserting the five electric heaters in the inside of the cylinder holes which is specified for these and make sure each heater works after each test.
3. Fixing the fin base (cylinder) after the fin installation on the steel arm.
4. Connecting the joint point of electric heaters to the power processing point of the voltage regulator device.
5. Installation of electrical connection (electric wire) of voltage regulator device to electrical power processing base.
6. Attaching the sensor of the surrounding temperature.
7. Numbering the thermocouples before the installation on the temperature recorder and after the installation on the body of the system.
8. Attaching the thermocouples to the temperature recorder.
9. Choosing one of the test fins to identify the seven thermocouple locations on the body of the double-triangular fin as shown in figure 3.16 following the following steps:

a- Determining the distance (20 mm) from the tip of the future rib of the fin (fin root or cylinder surface) towards the height of the fin and draw a straight line from this distance in the direction of the double triangular fin tendon (tip of the leaning rib of the fin) and then determine the distance (20 mm), (20 mm) and (20 mm), respectively from the fin upper root.

b- Identifying the intersection points of straight lines drawn from the root of the fin and from the bottom.

c- Doing a small mark at junction points before installing thermocouple.

d- Installing four thermocouples at the intersection point at the straight-line distance (20 mm) of the fin root and the straight-line distance (20 mm) of its lower end.

e- Installing thermocouple number (4) at the intersection point of the straight-line distance (20 mm) from the fin root tip and the straight-line distance.

f- Installing thermocouple number (5) at the intersection point of the straight-line distance (40 mm) from the fin root tip and the straight-line distance.

g- Installing thermocouple number (6) at the intersection point the straight-line distance (60 mm) of the fin root and the straight-line distance.

h- Installing thermocouple number (7) at the intersection point of the straight-line distance (80 mm) from the fin root tip and the straight-line distance.

10. Installing three thermocouples on the fin base cylinder as shown in Figure (3.15) following these steps:

a. Determining the middle of the fin base cylinder which is distance (1050 mm) from one end of the cylinder and work a circular line around the cylinder.

b. Making a straight line from the center of the cylinder so that the base of the cylinder is divided into two sections (semicircle) each.

c. Identifying three crossing points straight line center cylinder and mid fin base cylinder. Thermocouple (2) is installed at the center of the cylinder at (1050 mm).

d. Doing a small mark in the two predetermined locations as above and install the thermocouple (1) at the distance (20 mm) from the top and thermocouple (3) at the distance (20 mm) from the bottom of the cylinder base.

11. Installing one thermocouple in the air to measure the temperature of the surrounding air.

12. Connecting the electric wire of temperature recorder device to the base equipped with electrical power.

13. Switching on the base equipped with electrical power to operating mode for both voltage regulator device and temperature recorder in operating condition.

3.6.3. Test and Calculation Mechanism

The following procedures were followed in the implementation of the tests required in this study according to the coding used in Table (1.3). One case (Case I), which is similar to all other cases, which can be summarized in the following points:

1. Installing fins in their position on the cylinder base.
2. Putting electric heaters in their designated positions inside the fin base cylinder.
3. Putting the steel arm down the test sample after assembled.
4. Installing all thermocouples according to the assigned locations of the as mentioned earlier.
5. Choosing the first voltage by adjusting the voltage regulator and stabilizing it when carrying (91 volts) without operation.
6. Reading the current using its metering device.
7. Operating of temperature recorder and recording the measured temperature.
8. Operating of voltage regulator device.
9. After (90) minutes the necessary readings are taken from the voltage, current and temperature differentials of the previously mentioned thermocouples sites.
10. After selecting the second voltage (140V) leave the system for 60 minutes and then repeat steps (6), (7) and (8).
11. The process is restored in paragraph (9) at the third voltage (162V), the fourth (183 V) voltage and the fifth (190 V) voltage also at (60 minutes) each.
12. These paragraphs are repeated in all cases (I, II, and III) of testing that were previously coded.

3.7.The Study Cases

The work cases were divided into three cases: (I), (II), and (III). As shown in the Table below:

Cases	Status
Case I	The fin with drop 15 mm in the middle.
Case II	The fin with drop 35 mm in the middle.
Case III	The fin with drop 55 mm in the middle.

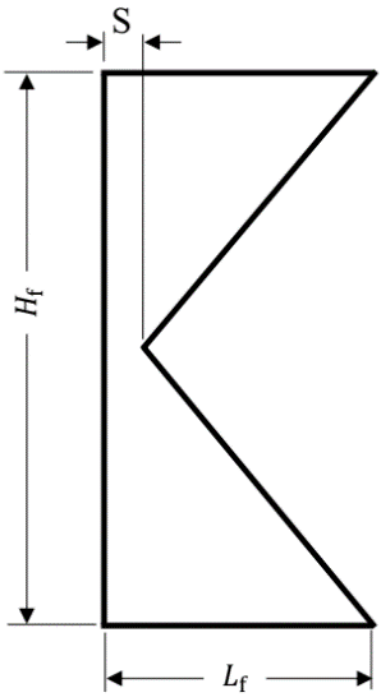

Figure 3.17: Double triangle fin.

Table 3.1: Dimensions of the geometric fin array for the cases under investigation.

	Heat sink		
	CASE I	**CASE II**	**CASE III**
H_f (mm)	210	210	210
L_f (mm)	105	105	105
S (mm)	15	35	55
t (mm)	3	3	3

3.8. Data Reduction

To determine the whole heat transfer rate of the heat sink, the radiation loss are measured and deducted from the total power provided by the heater. These are the precise details as follows:

$$q_{\text{in}} = \Phi \times I \tag{3.1}$$

$$q_{\text{convection}} = q_{\text{in}} - q_{\text{radiation}} \tag{3.2}$$

$$Q_{\text{radiation}} = F\sigma A\varepsilon(T_b^4 - T_\infty^4) \quad (3.3)$$

Where:

q_{in}: heat flux entering

Φ: Voltage

I: Electrical current

$q_{\text{convection}}$: Heat flux of convection

$q_{\text{radiation}}$: Heat flux of radiation

F: Form factor

σ: Stefan-Boltzmann constant 5.670*10^{-8}

A: Area

ε: Emissivity

T_b: Temperature of cylinder fin base.

T_∞: Air temperature

It has been estimated that less than 7% of the total heat has been lost through the experimental investigation.

Average temperature of cylinder surface can be calculated by:

$$T_b = \frac{1}{3}\sum_{i=1}^{3} T_{b,\text{i}} \quad (3.4)$$

The following format can be used to express the heat flux:

$$\dot{Q}_{\text{net}} = \frac{Q_{\text{convection}}}{A_b} \quad (3.5)$$

where (A_b) is the cylinder base area and expressed as:

$$A_b = 2\left(\frac{\pi}{4}D^2\right) + \pi D H_{\text{f}} - NH_{\text{f}}t - 5(\frac{\pi}{4}d_{\text{heater}}^2) \quad (3.6)$$

Where:

d_{heater}: electric heater diameter.

D: Diameter of fin base cylinder.

H_{f}: Fin height.

N: Number of fins.

t: Fin thikness.

The area of fin from Figure (3.13) which can be estimated as follows:

$$A_{\text{fin}} = 2\left[L_{\text{f}}H_{\text{f}} - \frac{1}{2}(L_{\text{f}} - S)H_{\text{f}}\right] + \left(2L_{\text{f}} + 2 \times \sqrt{(H_{\text{f}}/2)^2 + (L_{\text{f}} - S)^2}\right)t \quad (3.7)$$

Where:

A_{fin}: Area of the fin.

L_{f}: Fin length.

S: fin waist in (mm)

Consequently, the following equation may be used to get the heat transfer area:

$$A_{\text{net}} = A_b + NA_{\text{fin}} \quad (3.8)$$

Where:

A_{net}: Net area.

A_b: Area of the cylinder base.

This approach may be used to find the median free heat transfer coefficient:

$$h = \frac{Q_{\text{net}}}{A_{\text{net}}(T_b - T_\infty)} \quad (3.9)$$

Where h: Coefficient of heat transfer by convection.

The Nusselt number (*Nu*) can be expressed as:

$$Nu = \frac{hH_{\text{f}}}{k_{\text{air}}} \quad (3.10)$$

Where k_{air}: Air thermal conductivity.

Thus for the Rayleigh number (Ra) according to Eq. (3.11):

$$Ra = \frac{g\beta_{\text{air}}(T_b - T_\infty){H_{\text{f}}}^3}{\nu_{\text{air}}\alpha_{\text{air}}} \quad (3.11)$$

Where

g: Ground acceleration.

β_{air}: Volumetric expansion coefficient of the air.

ν_{air}: Kinematic viscosity of the air.

α_{air}: Thermal diffusivity of the air.

The heat sink thermal resistance is estimated using the experimental data as follows:

$$R_{th} = \frac{(T_b - T_\infty)}{Q_{net}} \quad (3.12)$$

Where R_{th}: Thermal resistance.

The current study is centered on free convection of the outer layer. The computations of the air characteristics were determined using the "Engineering Equation Solver (EES)" program. Comprehensive collection of variables suitable for inclusion in mathematical equations. (3.10) to (3.11) are evaluated at the bulk temperature. To determine how inaccurate the experimental results are, an uncertainty analysis is carried out. Errors in measurements can be random or systematic in nature. The temperature measurement accuracy error Φ_T is derived by the following calculation:

$$\Phi_T = t_{(N_{\text{data}}-1),95\%} \times \frac{\sigma_T}{\sqrt{N_{\text{data}}}} \qquad (3.13)$$

The variables *t*95%, σ_T, and N_{data} correspond to the *t* "the temperature's standard deviation (σT)", the number of data points, and the distribution at a 95% confidence level (N_{data}), and the degrees of freedom. The manufacturer's statement attributes the instrument's temperature measurement inaccuracy to the bias problem Ω_T.

$$\Omega_T = 0.26℃$$

The measurement of temperature uncertainty Ψ_T can be precisely defined as:

$$\Psi_T = \pm\sqrt{{\Omega_T}^2 + {\Phi_T}^2} \qquad (3.14)$$

Table (3.2) displays the calculated and displayed uncertainty of the temperature measurement Ψ_T. The measurement of the uncertainty of the thermal resistance Ψ_{Rth} has been defined as:

$$\frac{\Psi_{R_{th}}}{R_{th}} = \pm\sqrt{\left(\frac{\Psi_T}{T_b}\right)^2 + \left(\frac{\Psi_T}{T_\infty}\right)^2 + \left(\frac{\Psi_I}{I}\right)^2 + \left(\frac{\Psi_\phi}{\phi}\right)^2} \qquad (3.15)$$

The symbols Ψ_I and $\Psi\phi$ represent the uncertainty in the current and voltage measurements, respectively. The inquiry employs thermocouples with a precision of 0.03℃ and a data gathering system with a resolution of 0.1℃ and accuracy of ±(0.2%+0.1)℃, to measure temperatures at each location.

The measurement of the uncertainty of the thermal resistance Ψ_{Rth} has been defined as:

$$\frac{\Psi_{R_{th}}}{R_{th}} = \pm\sqrt{\left(\frac{\Psi_T}{T_b}\right)^2 + \left(\frac{\Psi_T}{T_\infty}\right)^2 + \left(\frac{\Psi_I}{I}\right)^2 + \left(\frac{\Psi_\phi}{\phi}\right)^2} \quad (3.15)$$

The symbols Ψ_I and $\Psi\phi$ represent the uncertainty in the current and voltage measurements, respectively. The inquiry employs thermocouples with a precision of 0.03℃ and a data gathering system with a resolution of 0.1℃ and accuracy of ±(0.2%+0.1)℃, to measure temperatures at each location.

Table (3.2) displays the calculated and displayed uncertainty of the temperature measurement Ψ_T.

Table 3.2: An overview of the uncertainty values.

Parameter	Uncertainty (%)
q_{in}	±6.33
Ra	±7.03
Nu	±4.46
R_{th}	±2.12

4. RESULT AND DISCUSSIONS

4.1. Introduction

The heat transmission properties of radial double triangular fins are investigated in this work. The experimental inquiry entailed conducting tests using various input heat rates, specifically 20.16, 66.03, 105.30, 157.62, and 196.08 W, using 12 fins. As mentioned earlier, numerous investigations have been carried out on rectangular and triangular fins. The temperature distribution plays a crucial role in heat transfer in various engineering applications (Bejan, 2003). The temperature distribution throughout the fin, as well as the thermal resistance and Nusselt number, have all been reported in this work. The findings were frequently displayed in the form of graphs, illustrating the correlation between temperature distribution and variables such as Nusselt number, thermal resistance, and fin height. To examine the temperature distribution at the fin base, several experiments were carried out.

4.2. Relationship of Change in Power Supplied (Thermal Flow) on Temperature Behavior

Figure (4.1) Depicts the correlation between the fin's height and the temperature difference resulting from various heat inputs. The experiment was carried out in three distinct circumstances. The temperature differential between the cylinder's surface and the ambient air is seen in the figure. The diagram depicts temperature distributions for different rates of input heat from the heating element. Since an increase in the input of heat causes a rise in the temperature gradient, the link between heat supply and temperature gradient is obvious. Nevertheless, the upward curve depicted in the figure signifies a decline in temperature within the laminar flow region. The second curve exhibits a pronounced decline, making it noticeably distinct from the other curves due to its proximity to the transitional region. The elevated heat input signifies a significant disparity in temperature. The larger surface area of the fins is what causes the large temperature disparity shown in example III.

The examination also evaluated the precise position of the thermocouples on the fin surface, specifically their height on the fin.

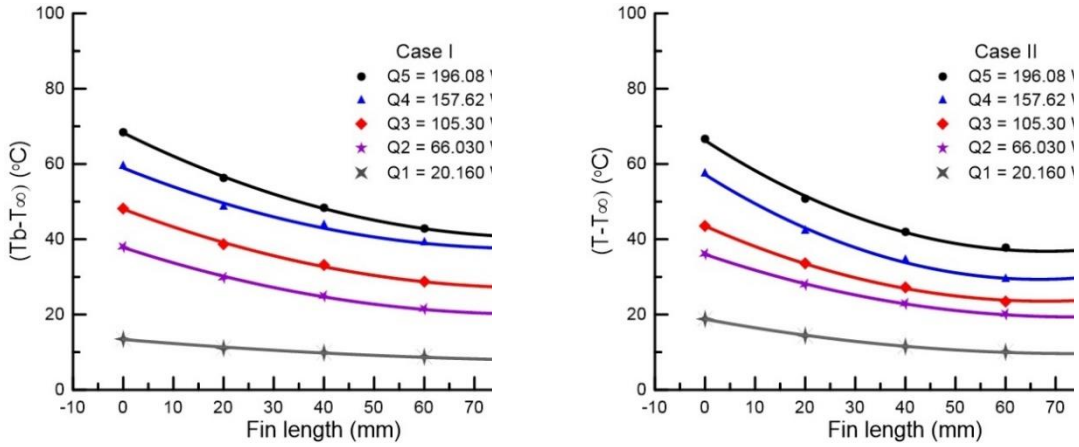

(a) case I (b) case II

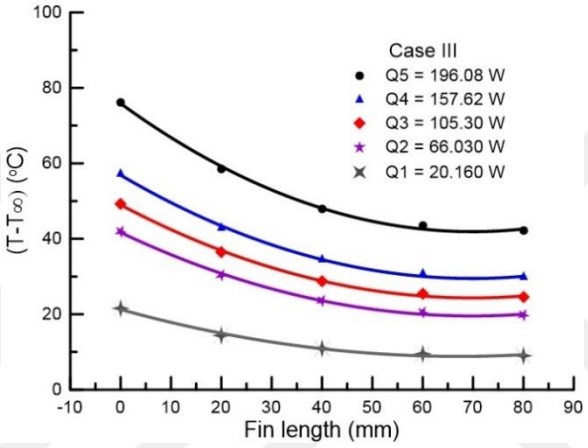

(c) case III

Figure 4.1: Temperature profiles analyzed for various fin heights and heat inputs in three different scenarios.

The examination also evaluated the precise position of the thermocouples on the fin surface, specifically their height on the fin. The connection between the radial heat sink's temperature and fin height for various heat input rates is shown in Figure (4.2), considering three different cases. The data illustrates the temperature of different surfaces in relation to the surrounding environment. Overall, as the height of the fin increases, temperatures fall for all the examples that were analyzed.

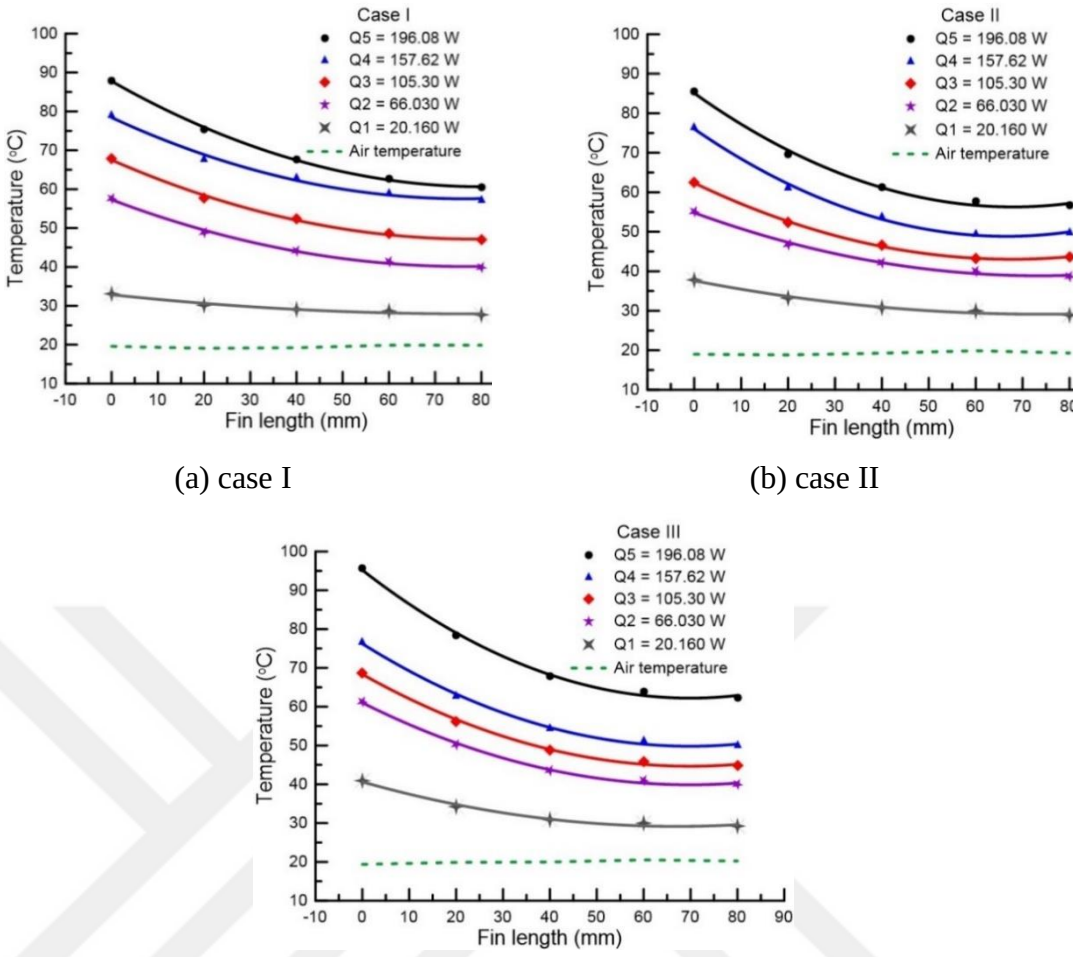

(a) case I (b) case II

(c) case III

Figure 4.2: The effect of fin height on temperature distribution in three studied cases.

The anticipated increase in air temperature under constant heat rates is delayed when air is present in and around a fin. In this approach, the air and fin temperatures are kept sufficiently separated to optimize the fin's heat-removal performance.

The link between the Nusselt number and the Rayleigh number for three particular case studies is shown in Figure (4.3). The Nusselt number exhibits a non-linear growth when the Rayleigh number grows in all examined circumstances. The figure clearly indicates that, when compared to the other experiments, example III's use of fins lowers the Nusselt number. The heat sink is in scenario I when the Nusselt number reaches its maximum value. The decline in the temperature differential between the fin base and the atmosphere around it, which is directly connected to the fins' decreasing surface area, is the cause of this phenomena.

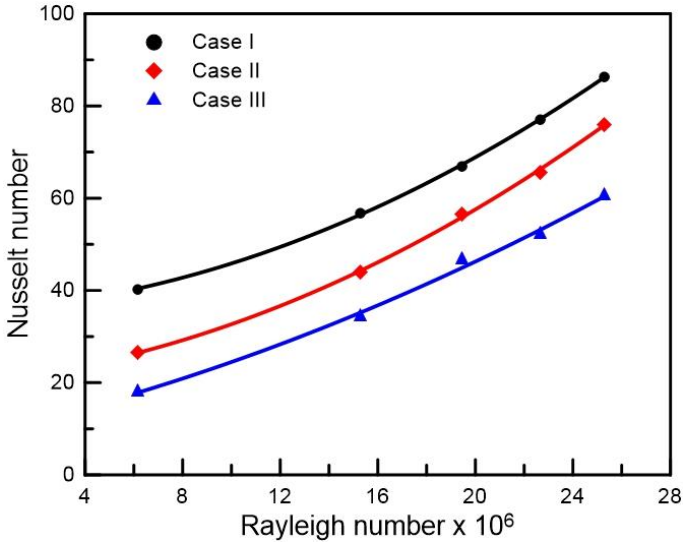

Figure 4.3: Examining the relationship between the heat sink's Nusselt number and the Rayleigh number under various conditions is the goal of this investigation.

4.3. Thermal Resistance

The effects of the source heat on the thermal resistance in different research settings are shown in Figure (4.4). The results show that when heat input rises in all analyzed scenarios, thermal resistance diminishes. As the amount of heat being applied grows, the resistance to heat flow decreases in a non-linear manner, as depicted in the figure. This can be elucidated by the augmentation of fluid flow. The heat transfer rate was improved and the heat sink thermal resistance was decreased by altering the fin design to enhance the area impacted by heat transfer. The increased fin surface area is responsible for this phenomenon.

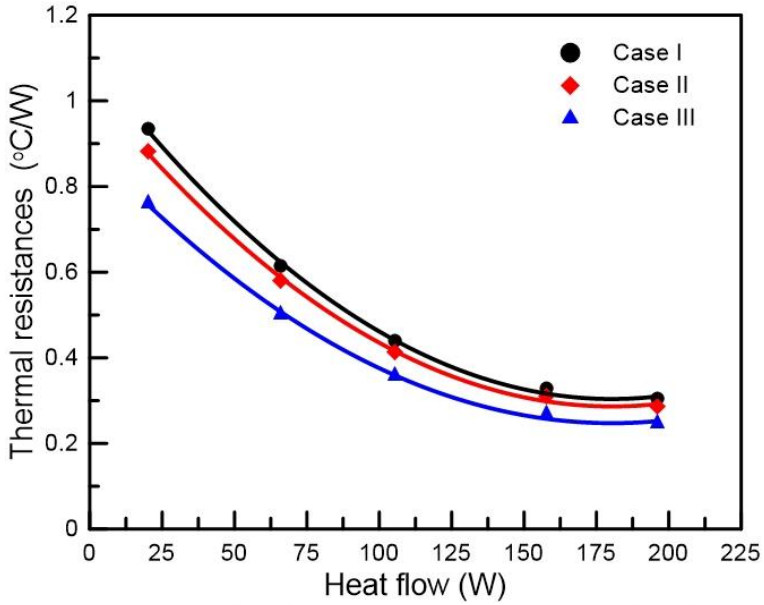

Figure 4.4: Variation in thermal resistance based on heat flow at several cases.

4.4. Nusselt Number

In order to build a reliable Nusselt number correlation, the functional form of the correlation is established from previous research. The cylindrical heat sink is surrounded by air currents that flow both vertically and horizontally. Put simply, a vertical flow that flows upward is caused by the heated fluid's force of buoyancy. The upward flow in the inner part is counteracted by a horizontal inward flow caused by the fluid from the surroundings. As a result, the overall flow pattern resembles the design of a chimney since it is composed of consecutive fins arranged on a level plane (Yu *et al*, 2010; Jang *et al*, 2014; An *et al*, 2012).

4.5. Developing The Correlation Equation

In this study, first an approximate of the Nusselt number correlation for the double rectangular fin arrangement on a flat surface has been made using its functional form. This functional form represents the Nusselt number correlation, which was derived from the study of (Harahap and McManus, 1967).

$$Nu = C\left(Ra\frac{A_{\mathrm{dir}}}{H_{\mathrm{f}}L_{\mathrm{f}}}\right)^{n_1}\left(\frac{P_{\mathrm{ave}}}{L_{\mathrm{f}}}\right)^{n_2}\left(\frac{H_{\mathrm{f}}}{L_{\mathrm{f}}}\right)^{n_3}\left(\frac{S}{L_{\mathrm{f}}}\right)^{n_4} \tag{4.1}$$

where, $RaA_{\mathrm{dir}}/H_{\mathrm{f}}L_{\mathrm{f}}$, $H_{\mathrm{f}}/L_{\mathrm{f}}$, and $P_{\mathrm{ave}}/L_{\mathrm{f}}$ denote the dimensionless fluid velocity, fin length, and fin-to-fin spacing, respectively. For a rectangular fin array on a horizontal surface, this correlation remains valid for the range of $1.61 \times 10^7 < RaA_{\mathrm{dir}}/H_{\mathrm{f}}L_{\mathrm{f}} < 6.62 \times 10^7$. Equation (4.1) represents the Rayleigh number (Ra), the

cross-sectional area of air flow (A_{dir}), and the average fin-to-fin spacing (P_{ave}). The (A_{dir}), also known as the projected area, and (P_{ave}), which represents the average perimeter, are determined based on the configuration of a radial heat sink with vertically aligned doubled triangular fins.

$$\left.\begin{aligned} A_{\mathrm{dir}} &= \pi(D/2 + L_{\mathrm{f}})^2 - \pi(D/2)^2 \\ P_{\mathrm{ave}} &= \pi(D + L_{\mathrm{f}})/N - t \end{aligned}\right\} \tag{4.2}$$

A least-squares fit is used to determine the Nusselt numbers derived from the experimental results in order to acquire the empirical coefficients C, n_1, n_2, n_3 and n_4.

$$C = 10.18, n_1 = 0.772, n_2 = -48.772, n_3 = -65.448, n_4 = -0.2772$$

we have

$$Nu = 10.18\left(Ra\frac{A_{\mathrm{dir}}}{H_{\mathrm{f}}L_{\mathrm{f}}} \times 10^{-6}\right)^{0.772}\left(\frac{P_{\mathrm{ave}}}{L_{\mathrm{f}}}\right)^{-48.772}\left(\frac{H_{\mathrm{f}}}{L_{\mathrm{f}}}\right)^{-65.448}\left(\frac{S}{L_{\mathrm{f}}}\right)^{-0.272} \tag{4.3}$$

The outcome of Equation (4.3) is depicted in Figure (4.5 a), revealing a maximum deviation of 7%, an average deviation of 4.8%, and a determination coefficient of R^2=97.3%. Eq. (4.3) fulfills the latter requirement, but the former condition is not relevant. In the present experiment, the correlation was adjusted in order to meet both criterion (Lee *et al*, 2016).

$$Nu = C\left(Ra\frac{A_{\mathrm{dir}}}{H_{\mathrm{f}}L_{\mathrm{f}}} \times 10^{-6}\right)^{n_1}\left(\frac{P_{\mathrm{ave}}}{L_{\mathrm{f}}}\right)^{n_2}\left(\frac{H_{\mathrm{f}}}{L_{\mathrm{f}}}\right)^{n_3}\left(1 - \frac{S}{L_{\mathrm{f}}}\right)^{n_4} \tag{4.5}$$

When the assumed coefficients are given as follows, the least-squares fitting approach shows that the corrected correlation nearly matches the Nusselt numbers obtained from the experiment data:

$$C = 1.227, n_1 = 0.771, n_2 = -0.01, n_3 = 1.581, n_4 = 0.667$$

Similarly:

$$Nu_L = 1.227\left(Ra\frac{A_{\mathrm{dir}}}{H_{\mathrm{f}}L_{\mathrm{f}}} \times 10^{-6}\right)^{0.771}\left(\frac{P_{\mathrm{ave}}}{L_{\mathrm{f}}}\right)^{-0.01}\left(\frac{H_{\mathrm{f}}}{L_{\mathrm{f}}}\right)^{1.581}\left(1 - \frac{S}{L_{\mathrm{f}}}\right)^{0.667} \tag{4.6}$$

Figure (4.5 b) illustrates the outcomes of Eq. (4.6), indicating that the highest and average discrepancies amount to 6.4% and 3.2% respectively. The coefficient of determination, denoted as R^2, is equal to 99.1%.

Another alternative connection to the Nusselt number, based on Eq. (4.7), is as follows:

$$Nu = C\left(Ra\frac{A_{\text{dir}}}{H_{\text{f}}L_{\text{f}}} \times 10^{-6}\right)^{n_1}\left(0.84 + \frac{100}{n_2}\left(\frac{P_{\text{ave}}}{L_{\text{f}}}\right)^{n_3}\right)^{-1}\left(\frac{H_{\text{f}}}{L_{\text{f}}}\right)^{n_4}\left(1 - \frac{S}{L_{\text{f}}}\right)^{n_5} \quad (4.7)$$

The coefficients that are empirical are provided in the expression:

$C = 4.043, n_1 = 0.771, n_2 = 2.835, n_3 = 2.351, n_4 = 3.428, n_5 = 0.667$

At the conclusion of the procedure, the correlation for the Nusselt number will be:

$$Nu = 4.043\left(Ra\frac{A_{\text{dir}}}{H_{\text{f}}L_{\text{f}}}\right)^{0.771}\left(0.88 + \frac{100}{2.835}\left(\frac{P_{\text{ave}}}{L_{\text{f}}}\right)^{2.351}\right)^{-1.5}\left(\frac{H_{\text{f}}}{L_{\text{f}}}\right)^{3.428}\left(1 - \frac{S}{L_{\text{f}}}\right)^{0.667} \quad (4.8)$$

The outcome of Equation (4.8), as depicted in Figure (4.5 c), reveals that the greatest deviation is 5.7% and the mean deviation is 3.1%. The coefficient of determination, denoted as R^2, is equal to 99.1%. Furthermore, these findings demonstrate a strong concurrence between the empirical data and the projected value.

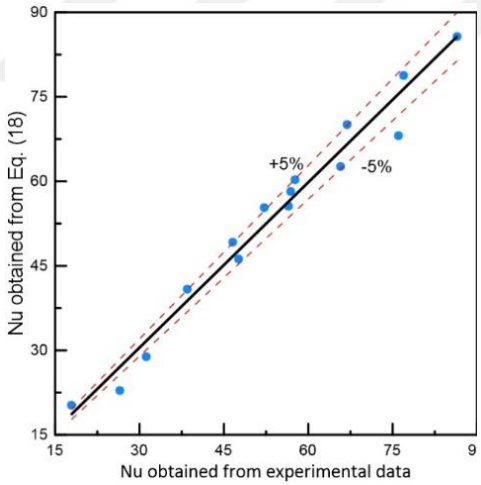

(a) Equation (4.4)

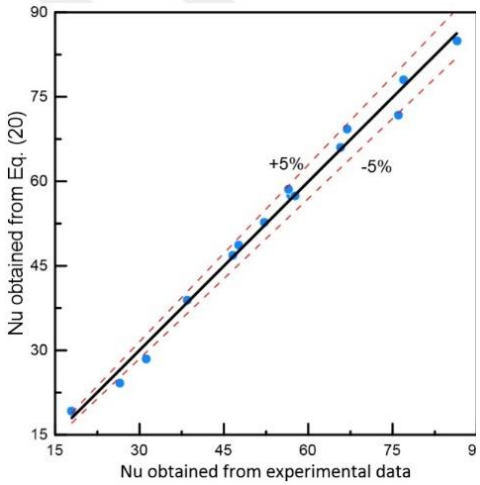

(b) Equation (4.6)

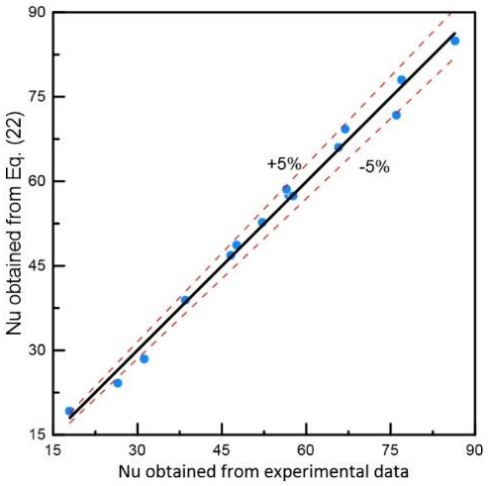

(c) Equation (4.8)

Figure 4.5: Comparison of the anticipated Nusselt numbers derived from the modified correlation with the measured Nusselt numbers acquired from experimental data.

The experimental study's findings are displayed in Table (4.1) below:

Table 4.1: Efficiency values along with fin height and the differences in added heat in the studied cases.

Thermocouple location		**T_1 (℃)**	**T_2 (℃)**	**T_3 (℃)**	**T_4 (℃)**	**T_5 (℃)**
Case I: Fin Drop = 15 mm						
V (volt)		91	140.2	160	183.5	190
I (A)		0.41	0.471	0.65	0.859	1.032
1	**Cylinder Surface (Base)**	33.78	56.1	68.95	80.5	89.44
2		33.21	54.87	66.64	79.15	87.55
3		32.28	55.73	67.77	77.26	86.93
4	**Fin**	30.16	45.88	54.76	64.58	69.7
5		29.09	44.11	52.28	63.85	67.6
6		28.66	43.36	51.57	60.58	65.75
7		27.7	39.89	46.97	59	58.92
8	**Air temp.**	19.59	19.08	19.22	19.87	19.87
Case II: Fin Drop = 35 mm						
V (volt)		91	140.2	160	183.5	190
I (A)		0.41	0.471	0.65	0.859	1.032
1	**Cylinder Surface (Base)**	38.19	57.15	62.73	80.19	86.16
2		38.75	55.99	61.94	79.19	85.92
3		36.52	54.19	58.43	77.28	84.66
4	**Fin**	31.87	43.75	47.59	57.06	62.6
5		30.8	42.15	46.55	55.76	61.24

6		29.99	41.65	44.16	52.4	60.64
7		28.91	38.7	43.66	50.73	58.71
8	**Air temp.**	18.99	18.83	19.27	19.89	19.31
Case III: Fin Drop = 55 mm						
V (volt)		91	140.2	160	183.5	190
I (A)		0.41	0.471	0.65	0.859	1.032
1	**Cylinder Surface (Base)**	41.36	62.96	64.15	74.45	100.45
2		40.86	61.59	62.15	73.82	99.34
3		40.56	59.26	61.39	72.33	98.23
4	**Fin**	31.24	43.4	44.25	48.66	62.55
5		30.96	42.55	43.87	47.5	61.7
6		30.4	41.99	42.47	46.28	61
7		30.23	40.79	41.87	44.78	60.97
8	**Air temp.**	19.36	19.88	19.98	20.5	20.23

The present study's findings were contrasted with those of an earlier investigation conducted by (Hassan *et al*, 2021) on test performance of radial triangular fins exposed to free thermal convection. The experimental work of this study included working conditions similar to the current working conditions where it highlighted the thermal performance of radial triangular fin, and the study included the use of three and six fins and the fragmentation of work into several cases: plane fins, perforated linear fins, randomly perforated fins) and then exposing these models to different voltages (70,110, and 160V), respectively, for specific time periods ranged between (60 and 90 minutes), using variable operational power supplied (25.69, 63.58, 136.96 W) respectively, to see how far this system can dissipate heat as the impact of engineering parameters has been studied (number of fins, shape of fins) in both cases on (thermal dissipation, Nusselt number, thermal efficiency and correlation coefficient). After obtaining readings through the devices and measurements used in this study, which used the same mathematical equations with the modification of other equations as our study identified in (Chapter Three) in order to obtain some important results of this test. The results of a specific case (six fins without perforation and the amount of heat equipped (136.96W of the above-mentioned study and compared to the results of our study) will be taken to compare the behavior of this case and try to find a scientific explanation for this case and show results to compare the following:

1. Heat exchange area in the case of six fins (0.16277 m^2) in the previous comparative study above. In our study, the heat exchange area if twelve fins with (15 mm waist) are installed (0.2128 m^2). The increase in the area exposed to heat exchange has

increased heat dissipation from air-prone surfaces and thus will result in lower temperatures being recorded at the fin base due to the large heat exchange area, which was the result of the adding additional fins, and this supports the effectiveness of increasing the area factor.

2. When studying the relationship of fin base temperature or cylinder wall (T_b) With the amount of heat supplied, we noticed that the fin base temperature in case of six fins at the voltage equipped (160V) and the amount of heat supplied (136.96W) temperature was measured to be (83.8℃) (in the previous comparative study). In our current study, using twelve fins, the temperature of the fin base was at voltage equipped (160V) and the amount of heat supplied (157.62W), the temperature reched (79.15℃), and we noticed that it increases by increasing the amount of heat supplied in all casesthis is because the relationship between temperature and heat supply is linear. It was also noticed that the highest temperatures were recorded at the six fins, this is due to the area of heat transfer was smaller than in the twelve fins. This could be considered as a good indiaction of our recent study due to the large heat exchange area, which was the result of the addition of more fins. This supports the effectiveness of the increase in the area factor, which represents any system whose heat and ambient air are to be dissipated, is important for the performance of such systems.
3. When studying the relationship of fin temperature (T_F) with the amount of heat supplied, we noticed that in the case of six fin as shown in (previous comparison study) at voltage equipped (160V) and at higher supplied capacity in the study (Q = 136.96W) were the lowest temperature values on the surface of the six-fin (50.1 ° C), while it had the highest temperature (65.2 °C), and at the supplied capacity of (Q = 157.62W) in our current research, the lowest temperature of the fin was (59.0 °C), while the highest temperature was (64.58 °C). Heat tranfer for all cases was under free convection conditions. The difference between the highest and the lowest temperatures is (5.58 °C). The main reason that temperatures differences in the case of twelve fins are lower is due to the surface area exposed to heat exchange being greater in the twelve fins than in the case of six fins, therefore, the heat dissipation is greater. It is clear that by increasing thermal flow temperatures will increase for all studied cases. The fin base region had the greatest temperature readings throughout the fin height, and the temperature decreased as we moved away from the fin base, the reason for this is that the fin base cylinder is the area closest to the heat source

and therefore the nearby areas that surround it are more affected than others, The gradient that gets in the temperatures due to the convection air-currents that try to cool the fins.

4. The highest value of the heat transfer coefficient recorded is as high as (19.89W/m^2.^{o}C) for six fins at at voltage equipped (160V) and the amount of heat equipped (136.96W) (in previous comparative study). While the heat transfer coefficient value in our current research has reached (10.18W/m2.^{o}C) for twelve fins at the same amount of heat supplied, it was noticed that increased supplied capacity has had a clear effect on the heat transfer coefficient in all tested cases. It was also shown that increasing the amount of heat equipped has increased the heat transfer coefficient. This is self-evident according to the equation of heat transfer by convection. Proportionality is a solitary proportion. Additionally, it was observed that in all of the scenarios that were analyzed, the regional heat transfer coefficient increased as the fin rose. This is due to the fact that as we move further from the fin base, the temperature differential between the ambient air and the fin surface, depending on its position, decreases, which in turn increases the temperature transfer factor according to the heat transfer equation of the free convection ($h = \frac{Q}{A\Delta T}$). In addition, the on-site heat transfer coefficient is increasing by increasing the amount of heat equipped and this is as obvious as in the above equation, since there is a strong correlation between the heat transfer coefficient and the quantity of heat equipped.
5. The relationship of thermal resistance with fin height and the change of heat equipped as the highest value recorded for thermal resistance ($R_{th} = 0.465$ ℃$/W$ in the previous comparative study) while thermal resistance recorded in our current study was ($R_{th} = 0.461$℃/W), generally speaking, heat resistance disposition was very similar in all six and twelve fins and appeared to us by studying all cases in the two studies without exception shows that thermal resistance is valued less by increasing the amount of heat processed, as heat resistance is related to($\frac{\Delta T}{Q}$) It becomes clear to us that there is an inverse relationship ($R_{th} \propto \frac{1}{Q}$) between thermal resistance and the amount of heat equipped. We found that the highest value of thermal resistance according to the heat capacity equipped at the surface of the base cylinder was in the case of six fins as shown above.

6. 6. For the six fins that were tested and attained, the Nusselt number value acquired (in the prior comparison research) was at the fin base (105), when the fitted capacity was maximum in the test which is (136.96W) while the Nusselt number in our current study was (77.11) at the equipped capacity. Perhaps the reason for this is that the coefficient of heat transfer by carrying (*h*) in the case of twelve fins is lower, as the coefficient of heat transfer (*h*) has a significant impact on the increase or decrease in the values of Nusselt number that can be obtained for the base of the fin.

4.6. A Sample of Calculation

Case I: Drop 15 mm

The voltage (Φ) of 160 volt

The current (I) of 0.65 A

The input electric power is:

$$q_{\text{in}} = \Phi \times I \tag{4.9}$$

$$q_{\text{in}} = 160 \times 0.65 = 104.0 \text{ W} \tag{4.10}$$

Average temperature of cylinder surface is:

$$\bar{T}_b = \frac{1}{3}\sum_{i=1}^{3} T_{b,\text{i}} \tag{4.11}$$

$$\bar{T}_b = \frac{1}{3}(\,68.95 + 66.64 + 67.77) = 67.79\ ℃ \tag{4.12}$$

The cylinder base area is:

$$A_b = 2\left(\frac{\pi}{4}D^2\right) + \pi D H_{\text{f}} - N H_{\text{f}} t - 5\left(\frac{\pi}{4}d_{\text{heater}}^2\right) \tag{4.13}$$

$$A_b = 2\left[\frac{\pi}{4}\left(\frac{70}{1000}\right)^2\right] + \pi\frac{70}{1000}\times\frac{210}{1000} - 12\frac{210}{1000}\times\frac{3}{1000} - 5\left[\frac{\pi}{4}\left(\frac{70}{1000}\right)^8\right]$$
$$= 0.045334 \text{ m}^2 \tag{4.14}$$

The heat flux is:

$$\dot{Q}_{\text{net}} = \frac{Q_{\text{in}}}{A_b} \tag{4.15}$$

$$\dot{Q}_{\text{net}} = \frac{104}{0.045334} = 2294.08 \ \frac{\text{W}}{\text{m}^2} \tag{4.16}$$

The fin area can be estimated as:

$$A_{\text{fin}} = 2\left[L_{\text{f}}H_{\text{f}} - \frac{1}{2}(L_{\text{f}} - B)H_{\text{f}}\right] + \left(2L_{\text{f}} + 2 \times \sqrt{(H_{\text{f}}/2)^2 + (L_{\text{f}} - S)^2}\right)t \tag{4.17}$$

$$A_{\text{fin}} = 2\left[\frac{15}{1000} \times \frac{210}{1000} - \frac{1}{2}\left(\frac{60}{1000} - \frac{15}{1000}\right) \times \frac{210}{1000}\right] + \left[2 \times \frac{210}{1000} + 2 \times \sqrt{\left(\frac{210}{2 \times 1000}\right)^2 + \left(\frac{60}{1000} - \frac{15}{1000}\right)^2}\right] \times \frac{3}{1000}$$

$$= 0.01396 \ \text{m}^2 \tag{3.24}$$

the net heat transfer area is:

$$A_{\text{net}} = A_b + NA_{\text{fin}} \tag{4.18}$$

$$A_{\text{net}} = 0.045334 \ + 12 \times 0.01396 = 0.2128 \ \text{m}^2 \tag{4.19}$$

The following equation yields the average free heat transfer coefficient:

$$h = \frac{Q_{\text{net}}}{A_{\text{net}}(\bar{T}_b - T_\infty)} \tag{4.20}$$

$$h = \frac{2294.08}{0.2128 \times (67.79 - 19.22)} = \ 10.062 \ \frac{\text{W}}{\text{m}^2\text{K}} \tag{4.21}$$

The appropriate air properties are calculated using the engineering equation solver (EES) program.

The air thermal conductivity is:

$$k_{\text{air}} = 0.0274 \ \frac{\text{W}}{\text{m K}} \tag{4.22}$$

The air kinematic viscosity is:

$$\nu_{\text{air}} = 1.58844 \times 10^{-5} \frac{\text{m}^2}{\text{s}} \tag{4.23}$$

The air thermal diffusivity:

$$\alpha_{\text{air}} = 2.2579 \times 10^{-5} \frac{\text{m}^2}{\text{s}} \tag{4.24}$$

The Nusselt number (Nu) is:

$$Nu = \frac{hH_{\mathrm{f}}}{k_{\mathrm{air}}} \tag{4.25}$$

$$Nu = \frac{10.062}{0.0274} \times \frac{210}{1000} = 77.117 \tag{4.26}$$

Rayleigh number is found by:

$$Ra = \frac{g\beta_{\mathrm{air}}(\bar{T}_b - T_\infty){H_{\mathrm{f}}}^3}{\nu_{\mathrm{air}}\alpha_{\mathrm{air}}} \tag{4.27}$$

The coefficient of thermal expansion:

$$\beta_{\mathrm{air}} = \frac{1}{\frac{[(\bar{T}_b + 273) + (T_\infty + 273)]}{2}} \tag{4.28}$$

$$\beta_{\mathrm{air}} = \frac{2}{[(67.79 + 273) + (19.22 + 273)]} = 0.00158 \tag{4.29}$$

Rayleigh number equation will be:

$$Ra = \frac{9.81 \times 0.00158 \times (67.79 - 19.22) \times \left(\frac{210}{1000}\right)^3}{1.58844 \times 10^{-5} \times 2.2579 \times 10^{-5}} = 19434871.39 \tag{4.30}$$

Thermal resistance is estimated by:

$$R_{th} = \frac{(\bar{T}_b - T_\infty)}{Q_{net}} \tag{4.31}$$

$$R_{th} = \frac{67.79 - 19.22}{2322.75} = 0.4612 \tag{4.32}$$

5. CONCLUSION AND RECOMMENDATIONS

5.1. Conclusion

A thorough analysis of natural convection in radial heat sinks with double triangular fins on either side was carried out. The study examines the effects of various heat rates on twelve fins and presents three unique instances, denoted as I, II, and III. The ensuing deductions are drawn:

- The Nusselt number exhibits a positive correlation with the Rayleigh number.
- The heat transfer dissipation in case I configurations was smaller than in case II and case III by 12.07% and 30%, respectively, at high Rayleigh numbers.
- The thermal resistance in instance III is lower than in case I and case II by 13.91% and 16.23%, respectively, at the maximum value of the Rayleigh number.
- The correlation of Nusselt number has high accuracy in predicting the real value (obtained by experimentation), with an error margin of less than ±5%, and a coefficient of determination (R^2) of up to 97%.
- The surface area of the extended surface and the fin's form design have the greatest effects on the temperature of the fin surface because, in test scenarios, the fin's surface area accelerates the process of heat dissipation from the fin base.
- Mass is an important factor in thermal systems such as extended surfaces, the larger the mass the higher the cost of production. It was observed that the lower the mass has been seen in the double-triangular fin with the most reduced waist. The highest mass reduction rate was observed in the case of fins with a drop of 15 mm in the middle and the lowest reduction rate was in the case of fin with a drop of 55 mm in the middle. Based on the foregoing, Reducing the bulk of the radial heat sink is mostly due to the increase in the intermediate hiding of the double triangular fins.
- The advancements achieved in this study have the potential to improve the geometric designs of extended surface thermal systems. The design of a double triangular radioactive heat sink for light-emitting diode (LED) light bulbs and the design of a radioactive heat sink with a similar pattern for numerous

engineering applications, including computer CPUs, are anticipated to benefit from the findings of this study.

5.2. Recommendations

From this study I can recommend some future studies as:

- Examining how the inclination angle affects the heat pump's performance.
- Studying the same configuration cooled laminar forced convection.
- Extending this study with numerical simulation.

6. REFERENCES

Ahmed, H. E., Salman, B., Kherbeet, A. S., & Ahmed, M. (2018). Optimization of thermal design of heat sinks: A review. *International Journal of Heat and Mass Transfer, 118*, 129-153.

Alam, M. W., Bhattacharyya, S., Souayeh, B., Dey, K., Hammami, F., Rahimi-Gorji, M., & Biswas, R. (2020). CPU heat sink cooling by triangular shape micro-pin-fin: Numerical study. International Communications in Heat and Mass Transfer, 112, 104455.

Al-Jamal, K., & Khashashneh, H. (1998). Experimental investigation in heat transfer of triangular and pin fin arrays. *Heat and Mass Transfer, 34*(2-3), 159-162.

An, B. H., Kim, H. J., & Kim, D.-K. (2012). Nusselt number correlation for natural convection from vertical cylinders with vertically oriented plate fins. *Experimental Thermal and Fluid Science, 41*, 59-66.

Aziz, A. (2006). Advanced heat conduction theory with a symbolic algebra package. In L. G. e. al. (Ed.), *Computational Methods* (pp. 829–848): Springer.

Baobaid, N.; Ali, M.I.; Khan, K.A.; Al-Rub, R.K.A. (2022). Fluid flow and heat transfer of porous TPMS architected heat sinks in free convection environment. Case Stud. Therm. Eng., 33, 101944.

Bejan, A. (2013). *Convection heat transfer*. (Fourth ed.). New York, USA: John Wiley & Sons Ins.

Bejan, A., & Kraus, A. D. (2003). *Heat transfer handbook*. New Jersey, USA: John Wiley & Sons, Inc.

Bergles, A. (2001). The implications and challenges of enhanced heat transfer for the chemical process industries. *Chemical Engineering Research and Design, 79*(4), 437-444.

Bergman, T. L., Lavine, A. S., Incropera, F. P., & Dewitt, D. P. (2011). *Introduction to heat transfer* (Sixth ed.). New York, USA: John Wiley & Sons. In.

Çengel, Y. A., & Ghajar, A. J. (2015). *Heat and mass transfer fundamentals & applications*. (Fifth ed.). New York, USA: McGraw-Hill Education.

Chu, W.-X., Lin, Y.-C., Chen, C.-Y., & Wang, C.-C. (2019). Experimental and numerical study on the performance of passive heat sink having alternating layout. *International Journal of Heat and Mass Transfer, 135*, 822-836.

Costa, V. A., & Lopes, A. M. (2014). Improved radial heat sink for led lamp cooling. *Applied Thermal Engineering, 70*(1), 131-138.

Dhanadhya, R. V., Nilawar, A. S., & Yenarkar, Y. L. (2013). Theoretical study and finite element analysis of convective heat transfer augmentation from horizontal rectangular fin with circular perforation. *International Journal of Mechanical and Production Engineering Research and Development, 3*(2), 187-192.

Dhumne, A. B., & Farkade, H. S. (2013). Heat transfer analysis of cylindrical perforated fins in staggered arrangement. *International Journal of Innovative Technology and Exploring Engineering, 2*(5), 225-230.

El Ghandouri, I., El Maakoul, A., Saadeddine, S., & Meziane, M. (2020). Design and numerical investigations of natural convection heat transfer of a new rippling fin shape. *Applied Thermal Engineering, 178*, 115670.

Elshafei, E. A. M. (2010). *Thermal Issues in Emerging Technologies*. Paper presented at the ThETA 3, Cairo, Egypt.

Enescu, D. (2019). Thermoelectric energy harvesting: basic principles and applications. *Green Energy Advances*, 1-20.

Faghri, A., & Zhang, Y. (2006). *Transport phenomena in multiphase systems*. Burlington, USA: Elsevier Inc.

Feng, S., Shi, M., Yan, H., Sun, S., Li, F., & Lu, T. J. (2018). Natural convection in a cross-fin heat sink. *Applied Thermal Engineering, 132*, 30-37.

Feng, S.; Shi, M.; Yan, H.; Sun, S.; Li, F.; Lu, T.J. Natural convection in a cross-fin heat sink. Appl. Therm. Eng., 132, 30–37.

Garimella, S. V., Fleischer, A. S., Murthy, J. Y., Keshavarzi, A., Prasher, R., Patel, C, Bhavnani, SH, Venkatasubramanian, R. M., & Ravi Joshi, Y. (2008). Thermal challenges in next-generation electronic systems. *IEEE Transactions on Components and Packaging Technologies, 31*(4), 801-815.

GOV, E. 2021. *LED lighting energy saver* [Online]. Available: https://www.energy.gov/energysaver/save-electricity-and-fuel/lighting-choices-save-you-money/led-lighting

Hahne, E., & Zhu, D. (1994). Natural convection heat transfer on finned tubes in air. *International Journal of Heat and Mass Transfer, 37*, 59-63.

Haldar, S. (2004). Laminar free convection around a horizontal cylinder with external longitudinal fins. *Heat Transfer Engineering, 25*(6), 45-53.

Haldar, S., Kochhar, G., Manohar, K., & Sahoo, R. (2007). Numerical study of laminar free convection about a horizontal cylinder with longitudinal fins of finite thickness. *International Journal of Thermal Sciences, 46*(7), 692-698.

Hanafi, M. Z. M., Ismail, F. S., & Rosli, R. (2015). Radial plate fins heat sink model design and optimization. In 2015 10th Asian control conference (ASCC) (pp. 1-5). IEEE.

Harahap, F., & McManus, H. N. (1967). Natural convection heat transfer from horizontal rectangular fin arrays. *Journal of Heat Transfer 89*,32-38.

Hassan, M. S., Weis, M. M., & Tahseen, T. A. (2021). Heat Transfer around a Radial Heat Sink with Triangular Fins Cooled by Natural Convection. Design Engineering, 16766-16784.

Huang, C.-H.; Chen, L. An optimized natural convection Y-shape-shifted heat sink design problem. (2021). Case Stud. Therm. Eng., 28, 101520.

Huang, C.-H.; Chen, W.-Y. A natural convection horizontal straight-fin heat sink design problem to enhance heat dissipation performance. (2018). Int. J. Therm. Sci. 2022, 176, 107540.

Iyengar, M., & Bar-Cohen, A. (1998). *Least-material optimization of vertical pin-fin, plate-fin, and triangular-fin heat sinks in natural convective heat transfer*. Paper presented at the ITherm'98. Sixth Intersociety Conference on Thermal and Thermomechanical Phenomena in Electronic Systems: p. 295-302.

Jang, D., Yook, S.-J., & Lee, K.-S. (2014). Optimum design of a radial heat sink with a fin-height profile for high-power LED lighting applications. *Applied Energy, 116*, 260-268.

Jang, D., Yu, S.-H., & Lee, K.-S. (2012). Multidisciplinary optimization of a pin-fin radial heat sink for LED lighting applications. *International Journal of Heat and Mass Transfer, 55*(4), 515-521.

Jassem, R. R. (2013). Effect the form of perforation on the heat transfer in the perforated fins. *Academic Research International, 4*(3), 198-205.

Johnston, E., Szabo, P. S., & Bennett, N. S. (2021). Cooling silicon photovoltaic cells using finned heat sinks and the effect of inclination angle. Thermal Science and Engineering Progress, 23, 100902.

Kazem, H. A., Al-Waeli, A. A., Chaichan, M. T., Sopian, K., & Al-Amiery, A. A. (2023). Enhancement of photovoltaic module performance using passive cooling (Fins): A comprehensive review. Case Studies in Thermal Engineering, 103316.

Khadke, R., & Bhole, K. (2018, February). Characterization of radial curved fin heat sink under natural and forced convection. In IOP Conference Series: Materials Science and Engineering (Vol. 310, No. 1, p. 012031). IOP Publishing.

Khan, W. A., Culham, J. R., & Yovanovich, M. M. (2006). The role of fin geometry in heat sink performance.

Kim, D.-K. (2012). Thermal optimization of plate-fin heat sinks with fins of variable thickness under natural convection. *International Journal of Heat and Mass Transfer, 55*(4), 752-761.

Kim, D.-K., Jung, J., & Kim, S. J. (2010). Thermal optimization of plate-fin heat sinks with variable fin thickness. *International Journal of Heat and Mass Transfer, 53*(25-26), 5988-5995.

Kraus, A. (1958). *The efficiency of a transistor cap as a heat dissipater*. Paper presented at the Proceedings of the 2nd National Heat Transfer Conference, ASME Chicago, IL., Pp. 1-15.

Kraus, A. D., Aziz, A., & Welty, J. (2001). *Extended surface heat transfer*. New York, USA: John Wiley & Sons, Inc.

Kumar, R. (1997). Three-dimensional natural convective flow in a vertical annulus with longitudinal fins. *International Journal of Heat and Mass Transfer, 40*(14), 3323-3334.

Kwak, D. B., Kwak, H. P., Noh, J. H., & Yook, S. J. (2018). Optimization of the radial heat sink with a concentric cylinder and triangular fins installed on a circular base. Journal of Mechanical Science and Technology, 32, 505-512.

Kwak, D. B., Noh, J. H., Lee, K. S., & Yook, S. J. (2017). Cooling performance of a radial heat sink with triangular fins on a circular base at various installation angles. International Journal of Thermal Sciences, 120, 377-385.

Lee, M., Kim, H. J., & Kim, D.-K. (2016). Nusselt number correlation for natural convection from vertical cylinders with triangular fins. *Applied Thermal Engineering, 93*, 1238-1247.

Lee, S. (1995). Optimum design and selection of heat sinks. *IEEE Transactions on Components, Packaging, and Manufacturing Technology: Part A, 18*(4), 812-817.

Leung, C. W., Probert, S., & Shilston, M. (1985). Heat exchanger design: thermal performances of rectangular fins protruding from vertical or horizontal rectangular bases. *Applied Energy, 20*(2), 123-140.

Li, B., Baik, Y. J., & Byon, C. (2016). Enhanced natural convection heat transfer of a chimney-based radial heat sink. Energy conversion and management, 108, 422-428.

Li, B., Jeon, S., & Byon, C. (2016). Investigation of natural convection heat transfer around a radial heat sink with a perforated ring. International Journal of Heat and Mass Transfer, 97, 705-711.

Li, J., & Yang, L. (2023). Recent Development of Heat Sink and Related Design Methods. Energies, 16(20), 7133.

Li, Y. F., Xia, G. D., Ma, D. D., Jia, Y. T., & Wang, J. (2016). Characteristics of laminar flow and heat transfer in microchannel heat sink with triangular cavities and rectangular ribs. International Journal of Heat and Mass Transfer, 98, 17-28.

Može, M., Nemanič, A., & Poredoš, P. (2020). Experimental and numerical heat transfer analysis of heat-pipe-based CPU coolers and performance optimization methodology. Applied Thermal Engineering, 179, 115720.

Muneeshwaran, M.; Tsai, M.K.; Wang, C.C. (2023). Heat transfer augmentation of natural convection heat sink through notched fin design. Int. Commun. Heat Mass Transf, 142, 106676.

Narendran, N., & Gu, Y. (2005). Life of LED-based white light sources. *IEEE/OSA Journal of Display Technology, 1*, 167–170.

Noda, H., Ikeda, M., Kimura, Y., & Kawabata, K. (2005). Development of High-Performance Heatsink "Crimped fin®". *Furukawa Review, 27*, 14-19.

Park, S.-J., Jang, D., Yook, S.-J., & Lee, K.-S. (2015). Optimization of a staggered pin-fin for a radial heat sink under free convection. *International Journal of Heat and Mass Transfer, 87*, 184-188.

Prakash, C., & Patankar, S. (1981). Combined free and forced convection in vertical tubes with radial internal fins. *Journal of Heat Transfer, 103*, 566-574.

Pua, S. W., Ong, K. S., Lai, K. C., & Naghavi, M. S. (2019). Natural and forced convection heat transfer coefficients of various finned heat sinks for miniature electronic systems. Proceedings of the Institution of Mechanical Engineers, Part A: Journal of Power and Energy, 233(2), 249-261.

Raithby, G. D., & Hollands, K. G. T. (1998). *Natural convection*. In: Rohsenow WM, Hartnett JP, Cho YI, (Eds.), Handbook of heat transfer. New York, USA: McGraw-Hill. Chapter 4; pp. 220-318.

Rao, A.K.; Somkuwar, V. (2021). Heat transfer of a tapered fin heat sink under natural convection. Mater. Today Proc, 46, 7886–7891.

Sadeghianjahromi, A., & Wang, C. C. (2021). Heat transfer enhancement in fin-and-tube heat exchangers–A review on different mechanisms. Renewable and Sustainable Energy Reviews, 137, 110470.

Sahin, B., & Demir, A. (2008). Performance analysis of a heat exchanger having perforated square fins. *Applied Thermal Engineering, 28*(5-6), 621-632.

Schnurr, N., & Cothran, C. (1974). Radiation from an array of gray circular fins of trapezoidal profile. *AIAA Journal, 12*(11), 1476-1480.

Schuepp, P. (1973). Model experiments on free-convection heat and mass transfer of leaves and plant elements. *Boundary-Layer Meteorology, 3*(4), 454-467.

Shaeri, M., & Yaghoubi, M. (2009). Thermal enhancement from heat sinks by using perforated fins. *Energy Conversion and Management, 50*(5), 1264-1270.

Shah, R. K. (2011). Extended surface heat transfer. In Thermopedia. Begel House Inc.

Shen, Q., Sun, D., Xu, Y., Jin, T., Zhao, X., Zhang, N., Huang, Z. (2016). Natural convection heat transfer along vertical cylinder heat sinks with longitudinal fins. *International Journal of Thermal Sciences, 100*, 457-464.

Stellman, J. M. (1998). *Encyclopedia of occupational health and safety* (Fourth ed.). Geneva, Switzerland: International Labour Organization.

Sundar, S., Song, G., Zahir, M. Z., Jayakumar, J. S., & Yook, S. J. (2019). Performance investigation of radial heat sink with circular base and perforated staggered fins. International Journal of Heat and Mass Transfer, 143, 118526.

Tari, I., & Mehrtash, M. (2013). Natural convection heat transfer from horizontal and slightly inclined plate-fin heat sinks. *Applied thermal engineering, 61*(2), 728-736.

Umrao Sarwe, D., & Kulkarni, V. S. (2021). Differential transformation method to determine heat transfer in annular fins. Heat Transfer, 50(8), 7949-7971.

Varma, E., & Gautam, A. (2022). A review of thermal analysis and heat transfer through fins. In AIP Conference Proceedings (Vol. 2413, No. 1). AIP Publishing.

Walunj, A., Daund, V., & Palande, D. (2014). Review of Performance of Rectangular Fins under Natural Convection at Different Orientation of Heat Sink. *International Journal of Innovation and Applied Studies*, *6*(2), 232-240.

Webb, R. L., & Kim, N.-H. (2005). *Principle of enhanced heat transfer* (Second ed.). New York, USA: Taylor & Francis.

Yildiz, Ş., & Yüncü, H. (2004). An experimental investigation on performance of annular fins on a horizontal cylinder in free convection heat transfer. *Heat and Mass Transfer, 40*, 239-251.

Yu, S.-H., Jang, D., & Lee, K.-S. (2012). Effect of radiation in a radial heat sink under natural convection. *International Journal of Heat and Mass Transfer, 55*(1-3), 505-509.

Yu, S.-H., Lee, K.-S., & Yook, S.-J. (2010). Natural convection around a radial heat sink. *International Journal of Heat and Mass Transfer, 53*(13-14), 2935-2938.

Yu, S.-H., Lee, K.-S., & Yook, S.-J. (2011). Optimum design of a radial heat sink under natural convection. *International Journal of Heat and Mass Transfer, 54*(11-12), 2499-2505.

CURRICULUM VITAE

Student Information	
Name/Surname:	JAMAL BAKR KHALEEL KHALEEL
Nationality:	IRAQ
Orcid No:	0009-0000-2429-5665

School Information	
Undergraduate Study	
University	TECHNICAL COLLEGE-KIRKUK-IRAQ
Faculty	TECHNICAL COLLEGE
Department	FUEL AND ENERGY
Graduation Year	2003
Graduate Study	
University	KIRŞEHİR AHİ EVRAN UNIVERSİTY
Institute	INSTITUTE OF NATURAL AND APPLIED SCIENCES
Department	DEPARTMENT OF MECHANICAL ENGINEERING
Graduation Year	2024

Articles and Papers Produced from the Thesis
Jamal bakr KHALEEL, Merdin DANIŞMAZ (2024), Experimental Investigation of Natural Convection Heat Transfer of A New Radial Double Triangular Fins Shape *International Scientific Research and Innovation Congress (oral presentation)*